

*Annual Review of Materials Research*

# Recent Advances in Understanding Diffusion in Multiprincipal Element Systems

Anuj Dash,<sup>1</sup> Alope Paul,<sup>1</sup> Sandipan Sen,<sup>2</sup>  
Sergiy Divinski,<sup>2</sup> Julia Kundin,<sup>3</sup> Ingo Steinbach,<sup>3</sup>  
Blazej Grabowski,<sup>4</sup> and Xi Zhang<sup>4</sup>

<sup>1</sup>Department of Materials Engineering, Indian Institute of Science, Bengaluru, India;  
email: aloke@iisc.ac.in

<sup>2</sup>Institute of Materials Physics, University of Münster, Münster, Germany

<sup>3</sup>Interdisciplinary Centre for Advanced Materials Simulation (ICAMS), Ruhr University  
Bochum, Bochum, Germany

<sup>4</sup>Institute for Materials Science, University of Stuttgart, Stuttgart, Germany

Annu. Rev. Mater. Res. 2022. 52:383–409

First published as a Review in Advance on  
April 28, 2022

The *Annual Review of Materials Research* is online at  
matsci.annualreviews.org

<https://doi.org/10.1146/annurev-matsci-081720-092213>

Copyright © 2022 by Annual Reviews.  
All rights reserved

## Keywords

diffusion, multiprincipal element alloys, tracer diffusion, interdiffusion, ab initio simulations, CALPHAD approach, pair-exchange model

## Abstract

Recent advances in the field of diffusion in multiprincipal element systems are critically reviewed, with an emphasis on experimental as well as theoretical approaches to determining atomic mobilities (tracer diffusion coefficients) in chemically complex multicomponent systems. The newly elaborated and augmented pseudobinary and pseudoternary methods provide a rigorous framework to access tracer, intrinsic, and interdiffusion coefficients in alloys with an arbitrary number of components. Utilization of the novel tracer-interdiffusion couple method allows for a high-throughput determination of composition-dependent tracer diffusion coefficients. A combination of these approaches provides a unique experimental toolbox to access diffusivities of elements that do not have suitable tracers. The pair-exchange diffusion model, which gives a consistent definition of diffusion matrices without specifying a reference element, is highlighted. Density-functional theory-informed calculations of basic diffusion properties—as

ANNUAL  
REVIEWS **CONNECT**

[www.annualreviews.org](http://www.annualreviews.org)

- Download figures
- Navigate cited references
- Keyword search
- Explore related articles
- Share via email or social media

required for the generation of extensive mobility databases for technological applications—are also discussed.

## 1. INTRODUCTION

Diffusion in multicomponent systems, particularly those systems where a principal component cannot be identified (i.e., multiprincipal element systems), is an intriguing transport phenomenon with many fundamental features and both experimental and theoretical challenges. Diffusion kinetics in general, and the analysis of diffusion-controlled processes in particular, are extremely important for both basic research and further development of industrial applications. Undoubtedly, diffusion in multiprincipal element alloys (usually with five or more elements), often called high-entropy alloys (HEAs), critically affects a number of crucial physical processes such as microstructural evolution, phase transitions, degradation, and mechanical properties at elevated temperatures (1).

HEAs are often available as simple (random) solid solutions such as face-centered cubic (FCC) CoCrFeMnNi (2), body-centered cubic (BCC) HfNbTaTiZr (3) or ZrNbTiVHf (4), and hexagonal close-packed (HCP) HoDyYGdTb (5) or  $\text{Al}_{15}\text{Hf}_{25}\text{Sc}_{10}\text{Ti}_{25}\text{Zr}_{25}$  (6) alloys, typically in a single phase state at higher temperatures. The relatively high thermal stability of such multiprincipal element solid solutions makes them ideal candidates for experimental and theoretical studies. Much of the fundamental diffusion-related research on these random alloys has been driven primarily by the concept of sluggish diffusion (7). The hunt for sluggish diffusion initiated many studies after the concept was hypothesized without thorough experimental verification. Since substitutional diffusion in typical metallic alloys is mediated by vacancies, one may modify the aim of this quest by asking whether the vacancy correlation factor—known to be just unity for self-diffusion in pure metals—is strongly reduced in HEAs. Such a hypothetical reduction would provide the fundamental reason for the sluggish diffusion phenomenon and thus clarify the hotly debated issue (8). However, although sluggish diffusion was postulated as one of the core properties of HEAs (7), so far, experimental studies have not supported this original hypothesis (8–10).

In this review, we first perform a comparative analysis of experimental measurements of the diffusion kinetics in HEAs. We demonstrate how the composition, type of crystalline lattice, and potential ordering phenomena affect the diffusion transport. We show that diffusion can be both reduced and enhanced by the multielement environment. Such measurements are in principle straightforward, though laborious, when utilizing the conventional radiotracer method. We summarize the understanding of various aspects of diffusion gained from this method. The conventional diffusion couple method cannot be practiced in multicomponent systems since the (one-dimensional) diffusion paths cannot be forced to intersect in the (multidimensional) multicomponent space. We demonstrate that newly proposed pseudobinary (PB) and pseudoternary (PT) methods circumvent this problem and thus can be applied in practice to these material systems. These methods have been shown to be efficient experimental approaches that allow for straightforward interpretation by producing physically reliable diffusion coefficients. The indirect estimation of tracer diffusion coefficients from these diffusion couple methods is also explained. Following this detailed experimental account, we focus on advances in theoretical investigations of diffusion in multiprincipal element alloys via state-of-the-art *ab initio* simulations. A general framework for the consistent assessment of diffusion parameters is presented. Finally, recent advances in calculation of phase diagrams (CALPHAD)-type modeling of diffusion phenomena in multiprincipal element systems are discussed. Thus, the whole spectrum of research is covered

---

**HEA:** high-entropy alloy

**PB:** pseudobinary

**PT:** pseudoternary

**CALPHAD:** calculation of phase diagrams

---

in this review, including accurate measurements of the diffusion parameters, fundamental understandings of the diffusion mechanisms, alloy thermodynamics, and short- and long-range order to technological applications in alloy development.

## 2. DIFFUSION IN MULTIPRINCIPAL ELEMENT SYSTEMS: FEATURES AND CHALLENGES

Diffusion transport in solids is commonly measured by using either the tracer technique (usually radiotracer) or chemical diffusion or interdiffusion couples (11). Tracer diffusion experiments are typically performed on a homogeneous alloy of a given composition where the isotope transport is driven by entropy. For example, self-diffusion measurements of Ni in an Ni-based alloy using the  $^{63}\text{Ni}$  tracer (12) correspond to a purely entropic driving force that governs the redistribution of the deposited marker atoms. In contrast, solute (impurity) diffusion of, for example, Cu in the Cu-free CoCrFeMnNi alloy using the  $^{65}\text{Cu}$  isotope (13) corresponds to chemical diffusion between the deposited film and the alloy. However, if the applied number of tracer atoms is vanishingly small, the measured chemical interdiffusion coefficients coincide with the solute tracer diffusion coefficients in the solute-free alloy (14). In both cases, the chemical potential gradients that constitute the most general driving forces are reduced to the concentration gradients of the applied tracer atoms. Correspondingly, the tracer diffusion coefficients of any element can conveniently be measured in an alloy with an arbitrary number of alloying components. The recent results for FCC, BCC, and HCP HEAs are critically reviewed in Section 3.

Chemical diffusion or interdiffusion is measured by bringing two different alloys in contact such that the atomic transport of the constituting elements is driven by the gradients of the chemical potentials. The interdiffusion coefficients can be determined straightforwardly for binary couples (in view of the Gibbs–Duhem relation, only one independent interdiffusion coefficient exists) along the whole interdiffusion path. In the case of ternary systems, the whole  $2 \times 2$  matrix of interdiffusion coefficients can be determined for the composition corresponding to the intersection of two diffusion paths (14). For a long time, it was common textbook knowledge that the interdiffusion matrix cannot be determined for quaternary and higher-order systems since it is experimentally impossible to enforce the intersection of three (or more) independent interdiffusion paths at a single composition in a high-dimensional compositional space (14). Only very recently have new breakthrough approaches been developed that seem to remove these longstanding limitations, as discussed in Section 4. Furthermore, a very new approach of radiotracer diffusion measurement in a concentration gradient (which had been proposed earlier but forgotten), a reliable measurement method of concentration-dependent tracer diffusion coefficients along the diffusion paths that develop in multicomponent couples, has been demonstrated (see Section 5).

Does high configurational entropy (due to an increased number of elements in a multicomponent alloy) retard substitutional diffusion? Self-diffusion in pure metals, known to be mediated by the random motion of vacancies, is well understood (11). Due to the different jump frequencies of different species, the vacancy jumps in random binary alloys are not fully random, forcing the corresponding vacancy correlation factor to be smaller than unity (15). Further, in a single-phase (solid solution) multiprincipal element alloy, the vacancy jumps are inherently biased by the local energy barrier disorder (see Section 6). For example, relatively large fluctuations of the energy barriers (about 0.5 eV) were predicted for Cr and Fe atoms in the equiatomic CoCrFeMnNi alloy (16). Deep pits in the potential energy landscape for vacancy migration might retard vacancy migration. A percolation threshold of about 19.8% for the FCC lattice was predicted in a binary alloy with mobile and immobile components (15). Note that this value nearly coincides with the concentration of a single component in a typical five-element HEA. Thus, one may expect the

vacancy correlation factor to depend strongly on the composition of such an alloy if the frequency of vacancy exchanges with one element exceeds those for all other components by many orders of magnitude.

However, the percolation threshold almost disappears in a binary alloy if the difference between the energy barriers for slow and fast diffusing species,  $\Delta E_m$ , is relatively small,  $\Delta E_m \leq 5kT$  (17). Taking a typical diffusion temperature of 1,300 K, the percolation concept would lose its importance for a typical random alloy if the difference between the energy barriers is  $\Delta E_m \leq 0.6$  eV. Otherwise, one may expect a certain retardation of the atomic transport in an HEA due to the strong correlations between successive vacancy jumps.

In the next sections, we analyze whether these predictions are relevant for the HEAs investigated so far.

### 3. TRACER DIFFUSION IN MULTIPRINCIPAL ELEMENT ALLOYS

Tracer diffusion measurement (with suitable radioactive or highly enriched natural isotopes) is one of the most powerful techniques to determine the tracer diffusion coefficients,  $D_i^*$  (directly related to the atomic mobilities,  $M_i$ ), of an element  $i$  in a given alloy of a certain composition (11). Typically, a chemically homogeneous alloy is used, and the determination of individual tracer diffusion coefficients for all constituting elements in a multicomponent alloy for a reasonably large number of compositions in an extended temperature interval represents a laborious and time-consuming task. This is why, so far, such measurements typically have been limited to pure metals (self-diffusion has not yet been measured for only a limited number of metals, for example, Ba), binary alloys, and (rarely) ternary alloys (18). Multiprincipal element alloys with five or more elements clearly pose a challenge to experimental capabilities.

In the following sections, we summarize and compare the measured tracer diffusion coefficients available so far for a collection of near-equiatomic HEAs possessing different compositions, lattice structures, and chemical and lattice ordering to demonstrate their respective roles in diffusion.

#### 3.1. The Role of Crystalline Lattices

Most of the tracer diffusion studies on HEAs reported so far have been performed on FCC systems (12, 13, 19, 20), with very few studies on BCC (21) or HCP (22) systems. It is still an open question whether the knowledge gained from FCC alloys can be transferred to other crystalline symmetries since diffusion in FCC HEAs has been measured in extended temperature intervals while that in BCC or HCP alloys has been measured only at representative temperatures (**Figure 1a**).

In **Figure 1a**, the tracer diffusion coefficients of representative constituent elements in HEAs of different crystalline symmetries are compared using the inverse homologous scale,  $T_m/T$ . Here  $T_m$  is the melting point of the corresponding alloy taken as the temperature corresponding to the maximum heat release during calorimetric measurements. The diffusion coefficients in different crystalline lattices are distinguished by colors, and self-diffusivities in pure metals, selected binary alloys, and HEAs are compared to determine the impact of configurational entropy on the diffusion rates of substitutional elements. In this figure, the Arrhenius plots are presented with typical uncertainties of the measured tracer diffusion coefficients being less than 20%. What is immediately evident from **Figure 1a** is that, at the same homologous temperature, the self-diffusivities in FCC systems are significantly smaller than those in BCC systems, which exhibit more obviously open structures that facilitate vacancy-mediated diffusion.

Self-diffusion in HCP systems is most intriguing. Whereas the reduced (i.e., scaled on the melting point) activation energies of self-diffusion in FCC and HCP pure metals are similar (11), Zr diffusion in the HCP HEA is significantly enhanced with respect to that in unary HCP metals,

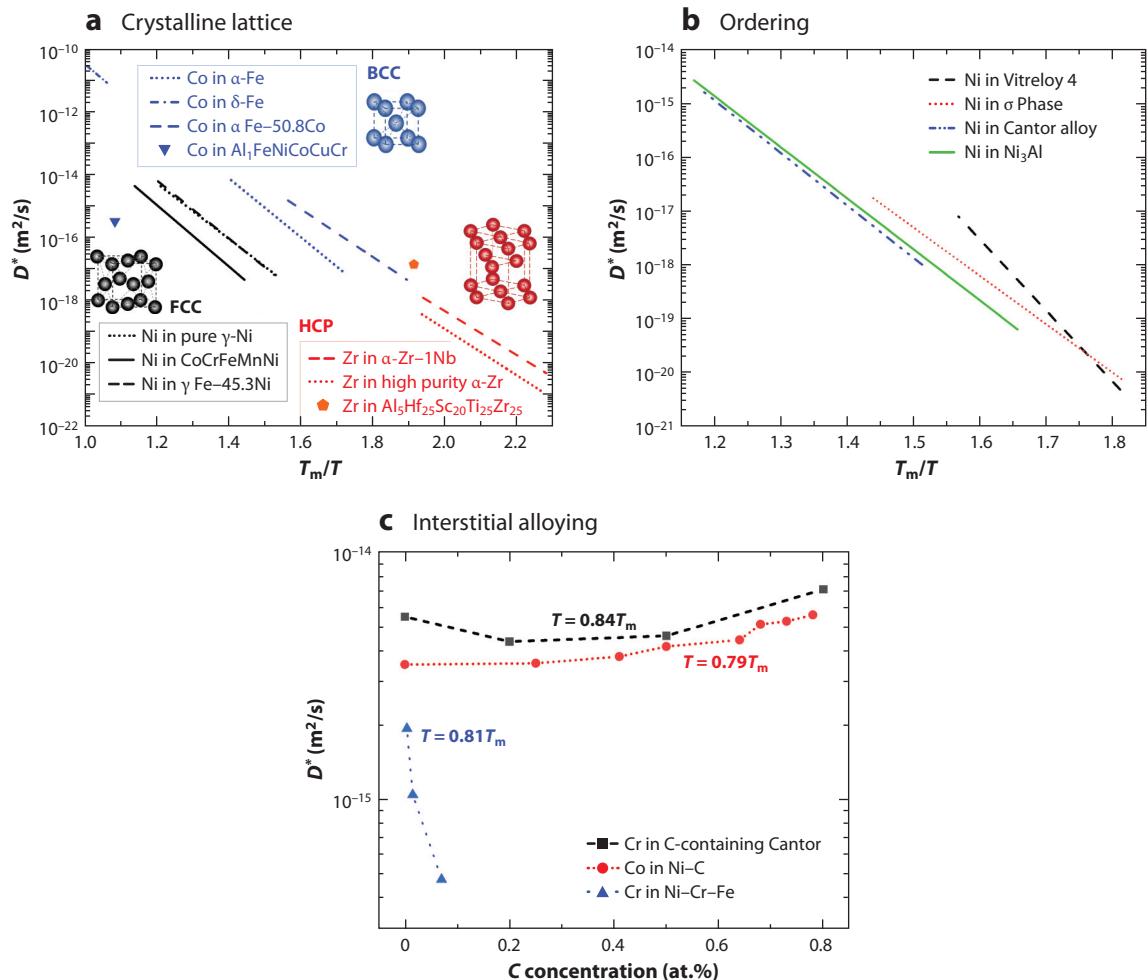


**Figure 1**

(a) Tracer diffusion coefficients,  $D^*$ , of selected constituting elements in FCC (Ni, *black lines*), BCC (Co, *blue lines*), and HCP (Zr, *red lines*) systems as the function of the inverse homologous temperature  $T_m/T$ . Corresponding diffusion rates are compared for pure elements [Ni (23),  $\alpha$ - and  $\delta$ -Fe (24), and  $\alpha$ -Zr (25)], binary alloys [ $\gamma$ -Fe-Ni (26),  $\alpha$ -Fe-Co (27), and  $\alpha$ -Zr-Nb (25)] and high-entropy alloys [CoCrFeMnNi (13), Al<sub>1</sub>FeNiCoCuCr (21), and Al<sub>5</sub>Hf<sub>25</sub>Sc<sub>20</sub>Ti<sub>25</sub>Zr<sub>25</sub> (22)].  $T_m$  is the melting point of the corresponding compounds. (b) Ni tracer diffusion coefficients  $D^*$  plotted as a function of homologous temperature  $T_m/T$  for different multicomponent systems with varying crystal structures: FCC CoCrFeMnNi HEA (13), Cr-rich  $\sigma$  phase (28), Ni<sub>3</sub>Al (29), and bulk metallic glass Vitreloy 4 (30). (c) The impact of interstitial carbon addition to various FCC systems on tracer diffusion of Co in binary Ni-C (31) and Cr in quaternary NiCrFe-C (32) and senary CoCrFeMnNi-C (33) alloys. The diffusivities are compared at about  $0.8T_m$ . The typical experimental uncertainties of the individual tracer diffusion coefficients are about 20%. For further information, one may refer to the original publications. Abbreviations: BCC, body-centered cubic; FCC, face-centered cubic; HEAs, high-entropy alloys; HCP, hexagonal close-packed.

although some retardation of diffusion is observed in FCC HEAs. In fact, the HCP systems show a very clear trend toward antisluggishness of diffusion induced by the multicomponent environment when analyzed on the homologous temperature scale. It has been reported that even minute amounts of impurities (such as of Fe or Co) present in technically pure  $\alpha$ -Ti or  $\alpha$ -Zr enhance the self-diffusion rates, especially at low temperatures (34). The most surprising finding,

however, is that Zr diffuses significantly faster, by orders of magnitude, in the nonequiatomic HCP Al<sub>15</sub>Hf<sub>25</sub>Sc<sub>10</sub>Ti<sub>25</sub>Zr<sub>25</sub> HEA than in unary Zr or binary Zr–Nb (**Figure 1a**). The reasons for such an enhancement are still to be determined.

Considering the FCC systems, self-diffusion of Ni in the CoCrFeMnNi Cantor HEA (13, 20) is slower than that in the unary Ni (23) and binary Fe–45.3Ni (26), suggesting a certain sluggishness of diffusion. The same sluggishness, however, does not seem to be true for the HCP systems.

Looking at the BCC systems, Co diffusion in AlCoCrFeNi (21) is significantly slower as compared with Co diffusion in paramagnetic  $\alpha$ - or  $\delta$ -Fe (24) with the BCC lattice. The Co diffusion rate in nearly equiatomic BCC Fe–Co alloys is enhanced with respect to that in pure Fe (**Figure 1a**) (21). One may anticipate a significant retardation of substitutional diffusion in BCC multiprincipal element alloys. However, the AlCoCrFeNi alloy features a two-phase with FCC and BCC/B2 structure (35), and the diffusivities reported in Reference 21 might be representative for the FCC component. Tracer diffusion measurements in single-phase BCC HEAs are required to shed light on the retardation or enhancement of diffusion induced by the multiprincipal element environment in the BCC lattice.

Following the arguments of Tsai et al. (36), one may suggest that diffusing vacancies experience different local mismatches between neighboring atoms and differences in bond strengths. Thus, fluctuations of lattice potential energies, which can affect vacancy migration via the multi-component matrix, are expected. Increasing the number of alloying components might increase these local fluctuations. Loosely speaking, one may hypothesize a reduction of atomic mobility as induced by increased configurational entropy. However, it is clearly not only increased configurational entropy that retards diffusion. Chemical disordering (associated with an increase of the configurational entropy) also enhances diffusion rates, at least in binary-ordered alloys (37).

Further analysis requires quantifying the distortions induced by multicomponent environments in HEAs. Normalized potential energy fluctuations,  $x_p$ , were proposed (10, 38) as being determined by the sum of elastic distortions,  $x_e$ , and chemical interactions,  $x_{ch}$ ,

$$x_p = x_e + x_{ch} = 4.12\delta\sqrt{\frac{\bar{K}\bar{V}}{k_B T}} + 2\left(\frac{\sqrt{\sum_i \sum_{j,j\neq i} (\Delta H_{ij}^{\text{mix}} - \bar{H})^2}}{k_B T}\right)^{1/2}, \quad 1.$$

where  $\delta = \sqrt{\sum_i (1 - \frac{r_i}{\bar{r}})^2}$  is the atomic distortion in an equiatomic alloy,  $r_i$  and  $\bar{r}$  are the atomic radius of element  $i$  and the mean atomic radius considering all the elements in the alloy, respectively,  $\bar{K}$  is the average bulk compressibility,  $\bar{V}$  is the atomic volume, and  $\Delta H_{ij}^{\text{mix}}$  and  $\bar{H}$  are the binary pair enthalpy of mixing elements  $i$  and  $j$  and the average enthalpy value for the alloy, respectively. In nonequiatomic alloys, all averaged values are taken as composition-weighted ones.

A simple comparison of the atomic radius mismatches for the HEAs in question ( $\delta = 1.6\%$ ,  $3.8\%$ , and  $7.2\%$  for FCC, BCC, and HCP alloys, respectively) suggests a strong impact of the elastic distortions on the sluggishness of diffusion in HEAs. In FCC CoCrFeMnNi alloys with a relatively small elastic mismatch, diffusion retardation due to an increasing number of components is observed. On the other hand, the diffusivity in the HCP AlHfScTiZr is increased. This behavior suggests a strong impact of the elastic distortions on substitutional diffusion in multicomponent alloys. Is this a pressure-like enthalpic term [i.e.,  $\exp(\sigma\Omega/k_B T)$ , with  $\sigma$  and  $\Omega$  being the local stress and activation volume of diffusion] or increased vibrational entropy at a higher level of elastic distortions? This question is yet to be answered. An absence of a clear correlation of the total  $x_p = x_e + x_{ch}$  value with the diffusion rate in a wide spectrum of FCC alloys has already been demonstrated (10). We conclude that increased potential energy fluctuations do not inevitably induce retardation of the diffusion rates.

### 3.2. The Role of Chemical and Crystalline Ordering

In **Figure 1a**, the Ni tracer diffusion coefficients in the disordered FCC CoCrFeMnNi Cantor alloy (13, 20), the  $\sigma$  phase of the  $\text{Co}_{17}\text{Cr}_{46}\text{Fe}_{16.3}\text{Mn}_{15.2}\text{Ni}_{5.5}$  alloy (28), the ordered  $L1_2$   $\text{Ni}_3\text{Al}$  (29), and bulk metallic glass Vitreloy 4  $\text{Zr}_{46.75}\text{Ti}_{8.25}\text{Cu}_{7.5}\text{Ni}_{10}\text{Be}_{27.5}$  (30) are compared using the homologous temperature scale. The comparison is made for the homologous temperatures where tracer diffusion coefficients were measured in the respective studies.

Comparing Ni self-diffusion in the CoCrFeMnNi multiprincipal element alloy with a simple FCC random solid solution with the ordered  $L1_2$   $\text{Ni}_3\text{Al}$  intermetallic compound and FCC-derived structure, it can be clearly observed that Ni diffuses in  $\text{Ni}_3\text{Al}$  at almost the same rate as in the Cantor CoCrFeMnNi alloy. The Ni diffusion mechanism in  $L1_2$ -ordered  $\text{Ni}_3\text{Al}$  is well-known (37) and corresponds to the sublattice diffusion mechanism. In  $\text{Ni}_3\text{Al}$ , vacancies are predominantly available on the Ni sublattice with a coordination number of eight, and Ni atoms diffuse via nearest-neighbor jumps over the Ni sublattice (37). One may speculate that the local chemical disorder in the CoCrFeMnNi alloy with the given spectrum of migration barriers for Ni atoms in particular is somehow equivalent to the decrease of the coordination number of Ni atoms from 12 to 8. In other words, a fraction of the crystallographic sites of the FCC lattice might be not accessible for diffusing Ni atoms due to relatively large associated migration barriers in the CoCrFeMnNi alloy.

The  $\sigma$  phase that is generally observed in Cantor and pseudo-Cantor systems at certain temperature ranges displays an enhanced Ni diffusivity as compared with the cubic systems. The crystalline lattice of the  $\sigma$  phase features five distinct sublattices with different occupation probabilities for different elements (28). The relative enhancement of Ni diffusion in the Cr-rich  $\sigma$  phase with respect to the equiatomic CoCrFeMnNi reference alloy has been explained by an increased vacancy concentration and decreased migration barriers due to the addition of Cr atoms instead of Ni ones (28). Nevertheless, density-functional theory (DFT)-informed input from theoretical analysis of diffusion in the  $\sigma$  phase is not yet available.

A bulk metallic glass, such as Vitreloy 4, is characterized by both chemical and crystalline disorder in view of the absence of the translational order. Below about  $0.6T_m$  (**Figure 1a**), Ni diffusion in the  $\text{Zr}_{46.8}\text{Be}_{27.5}\text{Ti}_{8.2}\text{Cu}_{7.5}\text{Ni}_{10}$  (Vitreloy 4) metallic glass becomes retarded and slowest among the given systems. At higher homologous temperatures, diffusion in the Vitreloy 4 is even faster than in crystalline lattices, probably due to their fundamentally different diffusion mechanisms. Note that a collective, string-like motion of groups of atoms has been suggested for diffusion in bulk metallic glasses (39), whereas substitutional diffusion in crystalline lattices is mediated by vacancies.

### 3.3. The Role of Interstitial Alloying

The impact of interstitial alloying, in particular C atoms, on the mobility of substitutional atoms has been recently investigated in detail (33). In **Figure 1c**, we compare the substitutional diffusion in binary Ni-C (Co diffusion) (31), quaternary Ni-Cr-Fe-C (Cr diffusion) (32), and senary CoCrFeMnNi-C alloys (Cr diffusion) (33) at about  $0.8T_m$ . Similar trends are generally seen for all investigated systems. The addition of C first decreases the substitutional diffusion rates; that is, the diffusion coefficients decrease slightly from the C-free alloy to alloys with 0.2% C (the effect is stronger in the Ni-Cr-Fe-C system). A further increase of the C concentration enhances the substitutional diffusion rates, which is explained by the increased vacancy concentration due to the induced lattice distortions (33). C atoms occupy interstitial sites with chemically different environments that induce local strains and might be responsible for the experimentally observed substitutional diffusion enhancement.

---

**DFT:**  
density-functional  
theory

---

## 4. ESTIMATION OF INTRINSIC AND TRACER DIFFUSION COEFFICIENTS FROM TERNARY AND MULTICOMPONENT DIFFUSION PROFILES

The radioisotope method demonstrated in the previous section is not possible to practice for the direct estimation of tracer diffusion coefficients of several components in ternary and multicomponent systems because of having either a short half-life (e.g.,  $^{32}\text{Si}$ ) or very costly radioisotopes (e.g.,  $^{26}\text{Al}$ ). The diffusion couple technique does not have these restrictions. However, this method faced a challenge in estimating diffusion coefficients experimentally in a multicomponent system. This challenge has recently been solved by newly proposed methods. These are first explained in ternary systems and then extended to the higher-order systems. A few new ideas are also proposed along with the methods already established.

The interdiffusion coefficients ( $\tilde{D}_{ij}^n$ ), interdiffusion flux ( $\tilde{J}_i$ ), and composition gradient ( $\frac{\partial N_i}{\partial x}$ ) of component  $i$  in an  $n$ -component system considering constant molar volume ( $V_m$ ) are related by (14, 40)

$$\tilde{J}_i = -\frac{1}{V_m} \sum_{j=1}^{n-1} \tilde{D}_{ij}^n \frac{\partial N_j}{\partial x}. \quad 2.$$

The interdiffusion flux of components can be calculated directly from the composition profiles (14). We need to estimate  $(n-1)^2$  independent interdiffusion coefficients in an  $n$ -component system at the composition of  $(n-1)$  intersecting diffusion paths in a multicomponent space. This is easy in a ternary system but almost impossible in a system with more than three components (40). The  $n(n-1)$  independent intrinsic diffusion coefficients are related to the interdiffusion coefficients by (40)

$$\tilde{D}_{ij}^n = D_{ij}^n - N_i \sum_{k=1}^n D_{kj}^n. \quad 3.$$

Based on Manning's formalism, the intrinsic diffusion coefficients ( $D_{ij}^n$ ) are related to the tracer diffusion coefficients,  $D_i^*$ , and thermodynamic factor,  $\theta_{ij}^n$ , by (41)

$$D_{ij}^n = \frac{N_i}{N_j} D_i^* \theta_{ij}^n + \xi N_i D_i^* \sum_{k=1}^{n-1} \frac{N_k}{N_j} (D_k^* - D_n^*) \theta_{kj}^n, \quad 4.$$

where  $\xi = \frac{2}{S_o \sum_{j=1}^n N_j D_j^*}$  and  $S_o$  is the structure factor (41, 42).

Darken (43) and Le Claire (44) neglected the cross-phenomenological terms of Onsager formalism (45, 46) to relate  $D_{ij}^n$  with  $D_i^*$  by only the first term. The second term of Manning's formalism is related to the vacancy-wind effect (41, 42), which may strongly influence certain intrinsic diffusion coefficients (47).

### 4.1. Ternary Systems

Only in binary systems can all types of diffusion coefficients be estimated by following the diffusion couple method, described in detail elsewhere (14). Following Equation 2, we need to estimate two main ( $\tilde{D}_{22}^1, \tilde{D}_{33}^1$ ) and two cross ( $\tilde{D}_{23}^1, \tilde{D}_{32}^1$ ) interdiffusion coefficients in a ternary system by considering, for example, component 1 as the dependent variable (48). We can estimate these parameters at the composition corresponding to the intersection of two diffusion couples. The interdiffusion coefficients are a kind of average of the intrinsic diffusion coefficients, which are related in Equation 3. However, the six intrinsic diffusion coefficients ( $D_{12}^1, D_{13}^1, D_{22}^1, D_{23}^1, D_{32}^1, D_{33}^1$ ) cannot be estimated in a ternary system by following the Kirkendall marker experiments. One can

easily intersect two diffusion profiles in a ternary system for the calculation of four interdiffusion coefficients. However, it is almost impossible to a priori predict the end-member compositions to find the Kirkendall marker plane at the composition of the intersection in both the diffusion couples (40) to solve six equations for the estimation of six intrinsic diffusion coefficients.

Kirkaldy & Lane (49) proposed a method of first estimating the tracer diffusion coefficients at the composition of the intersection in a ternary system, which then facilitates the calculation of intrinsic diffusion coefficients as well. We can substitute Equation 4 in Equation 3 to express the interdiffusion coefficients with respect to the tracer diffusion coefficients and the thermodynamic factors. Kirkaldy & Lane expressed the relations with respect to chemical potential gradients and van Loo and colleagues (50) expressed them with thermodynamic factors, which are material constants. With interdiffusion coefficients estimated from the composition profiles directly at the composition of the intersection and known thermodynamic factors, one can determine the tracer diffusion coefficients. Once the tracer diffusion coefficients are estimated, the intrinsic diffusion coefficients can be calculated utilizing Equation 4.

There are certain advantages to practicing the recently proposed PB diffusion couple technique over the method described above (8, 51–54). In this, the composition of one component (let us say component 3) is kept the same in the two end-members of a diffusion couple. When this component remains constant in the interdiffusion zone as well, such that only two components contribute to the diffusion profile, we can estimate the composition-dependent PB interdiffusion coefficient ( $\tilde{D}_{\text{PB}}$ ) over the whole composition range from a single diffusion couple (similar to the binary system) from (47)

$$\tilde{J}_i V_m = -\tilde{D}_{\text{PB}} \frac{\partial M_i}{\partial x}. \quad 5a.$$

As demonstrated extensively (47, 52, 53), two intrinsic diffusion coefficients,  $D_{22}^1$  and  $D_{11}^2$ , can be estimated directly from the composition profile at the Kirkendall marker plane following an augmented Darken–Manning approach, which is related by

$$\tilde{D}_{\text{PB}} = M_1^B D_{22}^1 + M_2^B D_{11}^2, \quad 5b.$$

where  $M_i^B = \frac{N_i}{N_1+N_2}$  is the modified composition relevant for the PB couple in a solid solution. The modified composition should be written differently in an intermetallic compound since components occupy different sublattices (55–57). The tracer diffusion coefficients can be calculated from (47)

$$D_{11}^2 = D_1^* [\theta_{11}^2 + M_1^B \xi_{\text{PB}} (D_1^* \theta_{11}^2 - D_2^* \theta_{22}^1)], \quad 6a.$$

$$D_{22}^1 = D_2^* [\theta_{22}^1 - M_2^B \xi_{\text{PB}} (D_1^* \theta_{11}^2 - D_2^* \theta_{22}^1)], \quad 6b.$$

where  $\xi_{\text{PB}} = \frac{2}{S_o \sum_{j=1}^2 M_j^B D_j^*}$  (47) and  $S_o$  is the structure factor (42).

One can also estimate the tracer diffusion coefficients at the intersecting composition of ternary and PB diffusion paths (see **Figure 2**). Two independent interdiffusion fluxes of a ternary diffusion couple can be expressed with the tracer diffusion coefficients and thermodynamic parameters by substituting Equations 3 and 4 in Equation 2. The interdiffusion flux of the PB couple can be expressed similarly by substituting Equations 5b, 6a, and 6b in Equation 5a. The tracer diffusion coefficients can then be calculated utilizing the thermodynamic parameters at the composition of the intersection. One can design the experiments such that several ternary diffusion paths intersect one PB diffusion path for estimation of the tracer diffusion coefficients systematically with the change in composition along the diffusion (composition) path of a PB couple (see **Figure 2**). Such

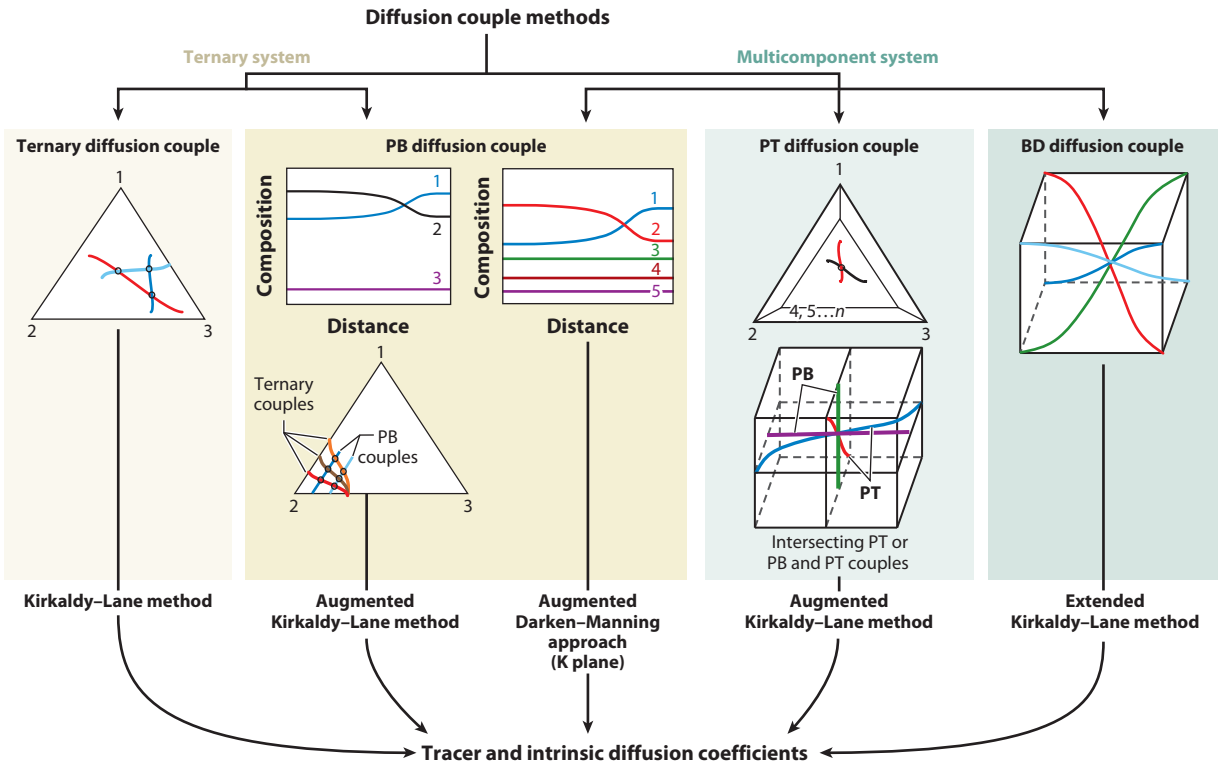


**Figure 2**

Estimations of tracer and intrinsic diffusion coefficients from different types of diffusion couple methods in the ternary and multicomponent systems are demonstrated. The data estimated at the cross of ternary diffusion paths may be generated at random compositions. Composition-dependent diffusion coefficients can be estimated systematically at the cross of pseudobinary (PB) and ternary diffusion paths. The PB diffusion couple methods can be followed in the ternary and multicomponent systems for estimation of composition-dependent interdiffusion coefficients over the whole composition range and intrinsic diffusion coefficients at the Kirkendall marker plane position. The pseudoternary (PT) method facilitates the estimation of both main and cross diffusion coefficients by intersecting the diffusion paths, which is otherwise not possible in a multicomponent space. One may estimate the diffusion coefficients following the body-diagonal (BD) diffusion couple method even when the diffusion couples do not intersect exactly. One may also estimate the diffusion coefficients at the cross of different types of diffusion paths.

systematic estimation is difficult a priori when intersecting only ternary diffusion paths because of the unknown serpentine nature of the ternary diffusion paths.

## 4.2. Multicomponent Systems

The estimation of diffusion coefficients in a multicomponent system is impossible by intersecting the diffusion paths (line profiles) in a multicomponent space (58). Morral (59) proposed the concept of the body-diagonal (BD) diffusion couple method in a small composition range of constant diffusivities with the possibilities of  $n - 1$  diffusion paths passing closely within different distances (instead of intersecting) for the estimation of  $(n - 1)^2$  interdiffusion coefficients (60). One might rather calculate tracer diffusion coefficients by extending the Kirkaldy-Lane method from only two diffusion couples with closest paths. Equations 3 and 4 can be substituted in Equation 2 to express the  $2(n - 1)$  interdiffusion fluxes with respect to the tracer diffusion coefficients, known thermodynamic factors, and composition gradients. A least squares method can then be used to

calculate the  $n$  tracer diffusion coefficients. Following this, one can calculate the intrinsic diffusion coefficients from Equation 4 and then the interdiffusion coefficients from Equation 3 (47).

As already explained, the PB diffusion couple method can be practiced in a multicomponent system by producing the diffusion couples such that only two components develop the diffusion profiles, keeping all other components constant (47, 52, 53). We have produced such ideal and near-ideal PB diffusion couples up to six or seven components. However, this method helps to estimate only the main diffusion coefficients. Therefore, the PT diffusion couple method was established in which a set of both main and cross-diffusion coefficients can be estimated (47, 61). With this method, only three components develop the diffusion profiles, keeping the other components constant. This restricts the diffusion paths on a two-dimensional plane (similar to the ternary system), and therefore, diffusion paths can be intersected. Considering that components 1, 2, and 3 develop the diffusion profiles, keeping all other components, 4– $n$ , as constant, four interdiffusion coefficients ( $\tilde{D}_{22}^1, \tilde{D}_{33}^1, \tilde{D}_{23}^1, \tilde{D}_{32}^1$ ) are estimated (similar to a ternary system). These are related to the six intrinsic diffusion coefficients ( $D_{12}^1, D_{22}^1, D_{32}^1, D_{13}^1, D_{23}^1, D_{33}^1$ ) by (47)

$$\tilde{D}_{ij}^1 = D_{ij}^1 - M_i^T (D_{1j}^1 + D_{2j}^1 + D_{3j}^1), \quad 7.$$

where  $M_i^T = \frac{N_i}{N_1+N_2+N_3}$ . This normalization of composition is different in the intermetallic compound, as explained in Reference 55. However, similar to the ternary system, these are very difficult to estimate following the Kirkendall marker experiments. To circumvent this problem, the augmented Kirkaldy–Lane method was developed for the PT couple (47). The intrinsic and tracer diffusion coefficients in a PT diffusion couple are related by (47)

$$D_{ij}^1 = \frac{M_i^T}{M_j^T} D_i^* \vartheta_{ij}^1 (1 + W_{ij}), \quad 8.$$

where  $1 + W_{ij} = 1 + \frac{2 \left( M_1^T D_1^* \frac{\vartheta_{1j}^1}{\vartheta_{1j}^1} + M_2^T D_2^* \frac{\vartheta_{2j}^1}{\vartheta_{2j}^1} + M_3^T D_3^* \frac{\vartheta_{3j}^1}{\vartheta_{3j}^1} \right)}{S_0 (M_1^T D_1^* + M_2^T D_2^* + M_3^T D_3^*)}$  is the vacancy-wind effect.

Therefore, one can estimate three tracer diffusion coefficients of the diffusing components by substituting Equation 8 into Equation 7 and calculating the tracer diffusion coefficients from the estimated interdiffusion coefficients and known thermodynamic parameters. We have found an excellent match between the data estimated by following this method and the radiotracer technique in the NiCoFeCr system (47, 53). Tracer diffusion coefficients of three and two components can be estimated from one type of PT and PB couple, respectively. Therefore, if possible, one can consider a set of intersecting PB and PT couples for estimation of the tracer diffusion coefficients of all the components (see **Figure 2**). This is found to be feasible in the NiCoFeCr system and can be practiced in other systems. With known tracer diffusion coefficients, one can estimate the intrinsic and interdiffusion coefficients of all the components (47).

Based on our analysis, an undetectable nonideality in the diffusion profiles of the components (which are supposed to remain constant) does not induce significant error into the calculations and such profiles can be treated as ideal PB or PT diffusion couples. Sometimes, these components may develop detectable but very minor diffusion profiles instead of remaining constant. By forcing the PB condition, one may still be able to calculate the PB diffusion coefficients with very minor errors. An extensive analysis is still required to analyze errors in the calculations, depending on the extent of the nonideality in these types of couples. An error analysis is also required in the BD couple method since the diffusion profiles do not intersect and induce an unknown error.

To summarize, a combination of different diffusion couple methods can be used to estimate the tracer, intrinsic, and interdiffusion coefficients. This method circumvents the limitations of radiotracer methods due to the absence of easy-to-handle radioisotopes of several elements (e.g., Al or Si) in various technologically important material systems.

### 4.3. Comparison of Tracer Diffusion Coefficients Determined by Different Methods

As mentioned above, there are two main approaches for experimentally determining the tracer diffusion coefficients of components in multiprincipal element alloys. The radiotracer method estimates these parameters directly from penetration depth profiles of tracer atoms. Thus, one can estimate the intrinsic diffusion coefficients (if required) by utilizing the thermodynamic details. On the other hand, tracer diffusion coefficients can also be estimated from the diffusion (composition) profiles developed in PB, PT, or BD diffusion couples utilizing thermodynamic details. Additionally, CALPHAD and numerical inverse methods are also utilized to extract the diffusion coefficients by optimizing the parameters to match the diffusion profiles. The data available in the literature for the nearly equiatomic CoCrFeNi alloy are compared in **Figure 3** (the error bars are specified when possible).

The data produced by Esakkiraja et al. (47) following the PB diffusion couple approach agree very well with the data produced by the radiotracer technique as performed by Gaertner et al. (13). A similar match was found when the data were estimated following the PT diffusion couple method (47) as well as in the data produced by Zhong et al. (63) following the numerical inverse method. Recently, Mehta et al. (64) estimated the Ni tracer diffusion coefficient of Ni in CoCrFeNi on the basis of linear response theory by coupling the Matano–Boltzmann approach and the Gaussian distribution function proposed by Belova et al. (65) to find a very good match with the data estimated by the direct radioisotope method (see **Figure 3**).

An important issue with the numerical inverse method is that different combinations of the atomic mobilities can potentially match the interdiffusion profiles, leading to unreliable output. These methods typically utilize thermodynamic details (63), and the availability of reliable data is very important. Thus, the uniqueness of the solution provided by a numerical inverse method may be an issue if the procedure is based solely on the concentration profiles. Recently, a novel numerical inverse method was developed without the use of thermodynamic parameters but uses the estimated intrinsic and interdiffusion coefficients as constraints in addition to the diffusion profiles for an exact solution (66).

## 5. TRACER DIFFUSION IN CONCENTRATION GRADIENTS: AUGMENTED TRACER-INTERDIFFUSION COUPLE TECHNIQUE

In his PhD thesis from the 1950s, Manning (67) proposed combining tracer and chemical diffusion measurements in a single experiment and addressing thermodynamic properties of the alloy. The corresponding experiments, carried out on binary Ag–Cd (67) and Ag–Au (68), were focused on the separation of the effects stemming from the vacancy flux and thermodynamic factors.

Almost 60 years later, Murch, Belova, and coauthors (65, 69) reanalyzed the original experiments and developed a framework for the rigorous determination of concentration-dependent tracer diffusion coefficients along the whole diffusion path that is produced in a binary couple. The proposed experimental approach was then further elaborated by Gaertner et al. (62) and applied to diffusion measurements in a multicomponent  $\text{Co}_{15}\text{Cr}_{20}\text{Fe}_{20}\text{Mn}_{20}\text{Ni}_{25}/\text{Co}_{25}\text{Cr}_{20}\text{Fe}_{20}\text{Mn}_{20}\text{Ni}_{15}$  couple. Recently, the augmented tracer-interdiffusion couple approach has been successfully utilized to assess concentration-dependent Ga tracer diffusion coefficients in binary Fe–Ga couples by measuring the tracer diffusion of the  $^{59}\text{Fe}$  isotope in the corresponding concentration gradients (70).

The augmented tracer-interdiffusion couple approach is sketched in **Figure 4**. A tracer isotope [in this particular case, the  $^{59}\text{Fe}$  radioisotope (70)] is applied to both of the opposite surfaces of each half of the diffusion couple before the samples are brought in contact. After annealing, the

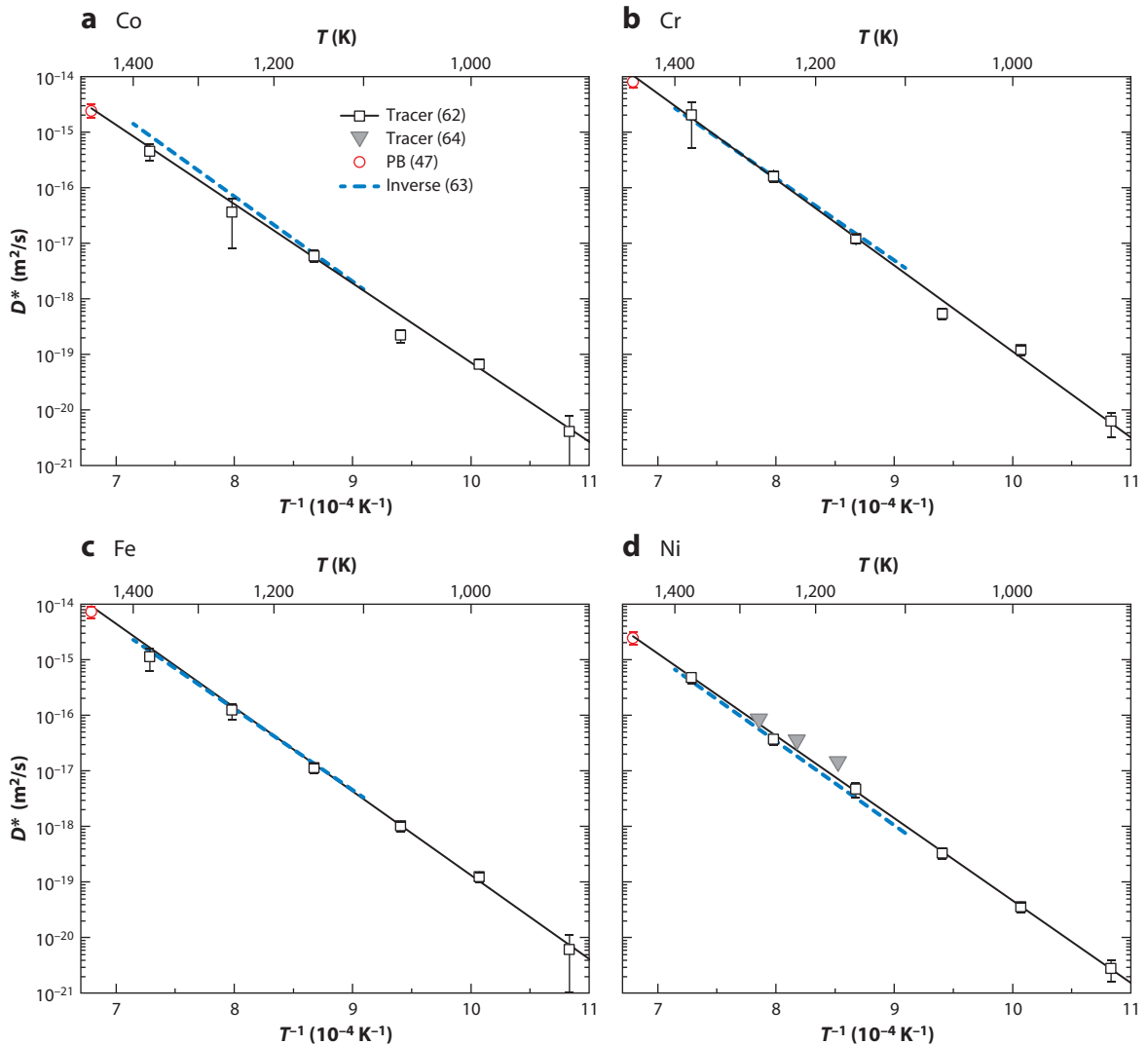


**Figure 3**

The tracer diffusion coefficients of (a) Co, (b) Cr, (c) Fe, and (d) Ni in nearly equiatomic CoCrFeNi HEAs determined by the direct radiotracer diffusion measurements (squares, black solid lines) (62), the PB diffusion couple method (red circles) (47), and a numerical inverse scheme (blue dashed lines) (63). The tracer diffusion coefficients of Ni as determined by Mehta et al. (64) are shown as triangles. Abbreviations: HEAs, high-entropy alloys; PB, pseudobinary.

diffusion couple is sectioned through and the tracer concentration profile is determined (Figure 4a). An identical couple is cross sectioned and the element concentration profile is measured using electron microprobe analysis (Figure 4c). Having determined both tracer and chemical concentration profiles, the tracer diffusion coefficient is then determined as a function of the composition (Figure 4d). The tracer diffusion coefficients are independently measured in two end-members with homogeneous compositions as well. The consistency of the whole data set underlines the correctness of the approach (62, 70). In the case of the binary couple, the interdiffusion coefficient can be determined as well (Figure 4d). If the approach is applied to a

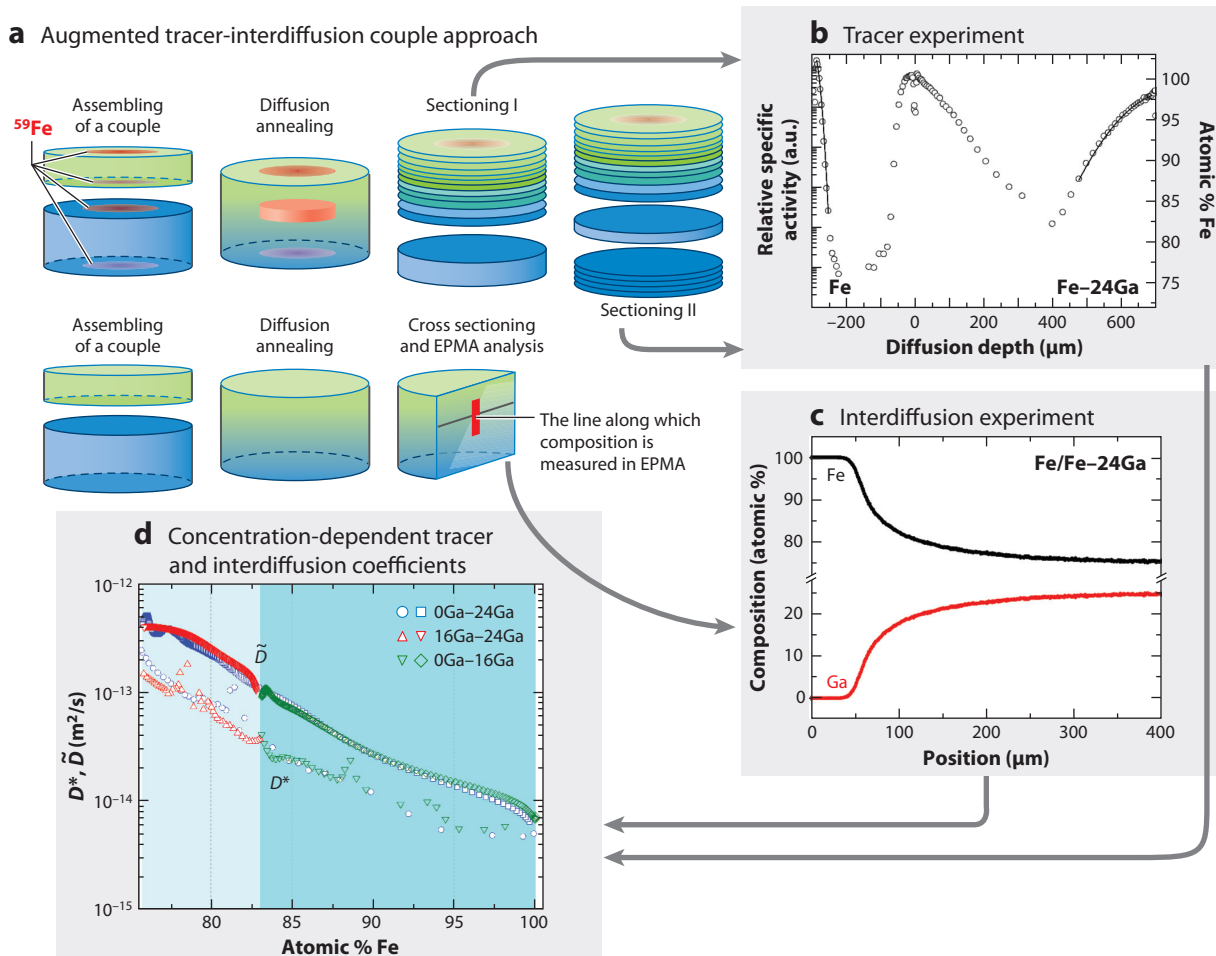


**Figure 4**

A schematic representation of the augmented tracer-interdiffusion method in application to the Fe–Ga system. The radiotracer experiment is combined with the diffusion couple method for estimation of both composition-dependent tracer and interdiffusion coefficients. This facilitates estimation of the tracer diffusion coefficient of an element that does not have a suitable radioisotope from the tracer diffusion coefficient of another element that has a suitable radioisotope for tracer diffusion experiments and interdiffusion coefficients. Different shades of blue and green in panel *a* and different shades of blue in the background in panel *d* represent different composition ranges. For further details, see the work of Muralikrishna et al. (70). Abbreviation: EPMA, electron probe microanalysis.

PB couple in a multicomponent alloy, the tracer diffusion coefficients and the PB interdiffusion coefficients can be determined. In the case of an arbitrary multicomponent couple, only tracer diffusion coefficients (as a function of the concentration along the developed diffusion path) will be determined (62).

The augmented tracer-interdiffusion couple method allows a consistent determination of the concentration-dependent tracer diffusion coefficients in general diffusion couples along whole interdiffusion paths in multicomponent alloys (including the end-members). The independent tracer diffusion measurements in the unaffected end-members help to overcome common difficulties with correctly determining the concentration gradients and the integration of the concentration profiles near the end-member compositions.

The combination of PB or PT couples (see Section 4) with the tracer-interdiffusion method offers unprecedented advantages for accessing the tracer and interdiffusion (as well as intrinsic) coefficients in the same couples. In the case of existing thermodynamic descriptions, the tracer diffusion coefficients of elements for which no suitable radioisotopes exist could be determined. The PB and PT approaches allow independent determination of the tracer diffusion coefficients that again provides access to atomic mobilities of the chemical elements with no suitable radioisotopes (e.g., Al or Ga in Reference 70).

## 6. AB INITIO SIMULATIONS OF DIFFUSION IN MULTICOMPONENT SYSTEMS

As discussed in previous sections, various diffusion coefficients in HEAs are experimentally accessible via the diffusion couple or radiotracer techniques, including the newly developed tracer-interdiffusion couple approach. The composition- and/or temperature-dependent diffusion rates can be utilized to extract diffusion parameters such as the activation energies and the prefactors. This information, however, provides only limited physical insight into the related diffusion mechanisms behind the observed phenomena given it is prone to large uncertainties when the measurements are done within experimentally accessible temperature intervals. Tracer experiments especially focused on, for example, pressure dependence or isotope effects (11) are required. Theoretical predictions, especially based on state-of-the-art, ab initio DFT simulations, provide an alternative approach to obtaining the diffusion rates and diffusion properties. An attractive bonus offered by such simulations, beyond the mere calculated diffusion data, is a thorough microscopic understanding of the observed phenomena. Moreover, DFT-informed calculations may provide unique access to the diffusion parameters in the metastable phases that are also required for CALPHAD-like modeling (see Section 7).

Ab initio prediction of diffusivities and related properties in low-order systems (e.g., pure metals or binary alloys in the dilute limit) has become commonplace. For self- and solute diffusion in pure metals and dilute alloys, excellent agreement with high-temperature experimental data can be achieved, provided that the relevant thermal excitation effects are taken into account as the configurational degrees of freedom are very limited. Going beyond the well-established quasi-harmonic approximation, accurate and efficient ab initio methodologies for explicit anharmonicity have acquired maturity and have shown great success in recent years. However, the ab initio computational framework utilized for diffusion in pure metals and dilute alloys breaks down for concentrated multicomponent alloys due to their explosive configurational space. In such alloys, the energetics relevant for diffusion simulations, such as the formation and migration energies of vacancies or interstitial defects, becomes very sensitive to the chemical environment. The chemical environment may also have a strong impact on the vibrational degrees of freedom, further increasing the challenges of exploring diffusion in concentrated multicomponent alloys. In the following subsections, we present recent methodological developments that address the diffusion energetics related to both configurational and vibrational degrees of freedom in multicomponent systems. We also introduce approaches to extract various diffusion coefficients. Finally, possible future developments are suggested and discussed.

### 6.1. Coarse-Graining Configurational Space for Defect Diffusion Energetics

From the atomistic perspective, we mainly focus in this review on substitutional (vacancy-mediated) and interstitial (impurity atoms) bulk diffusion as these diffusion mechanisms are generally the dominant ones. Among the key quantities that are necessary to calculate the diffusion rates and to understand the involved physics are the defect diffusion energies (i.e., the formation

---

**DOS:** density of states

**SQS:** special  
quasirandom structure

**CE:** cluster expansion

---

and migration energies of the defects). The formation energies in particular determine the concentration or solubility of the defects. In general, the chemical configuration in the vicinity of a defect has a strong impact on the formation and migration energies of defects. The resulting effective energetics must be extracted on the basis of a statistical analysis with the knowledge of the distribution of individual defect energy states, that is, the density of defect states (defect DOS) describing the number of defect states with a formation energy within a small energy interval. Unlike in pure metals or dilute alloys where defects are associated with a small number of local atomic environments, *ab initio* modeling of defect properties in concentrated multicomponent alloys faces significant challenges as the number of chemical environments combinatorially explodes with the number of components. In order to achieve sufficient statistics for sampling the defect DOS, different coarse-graining approaches can be applied. We mainly discuss here DFT-based *ab initio* approaches.

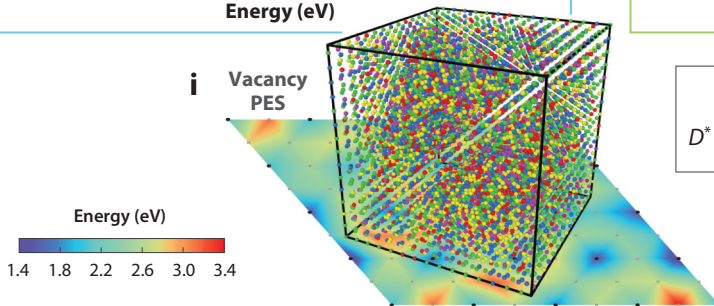
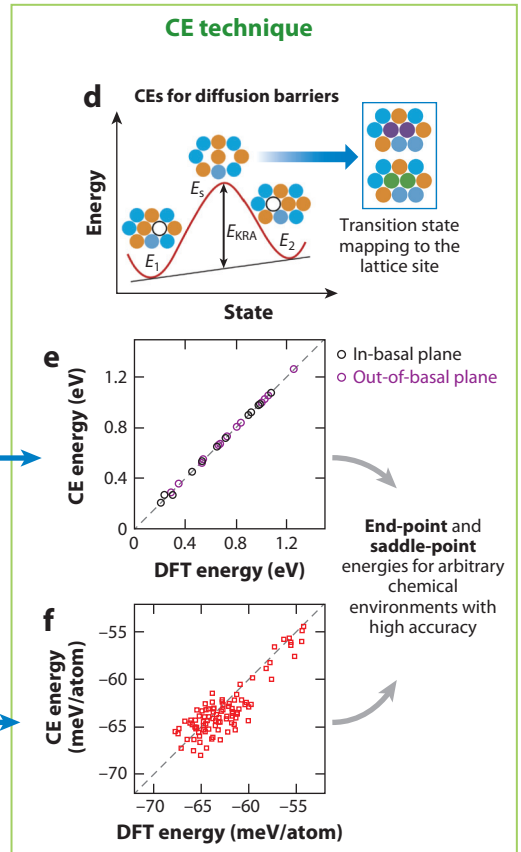
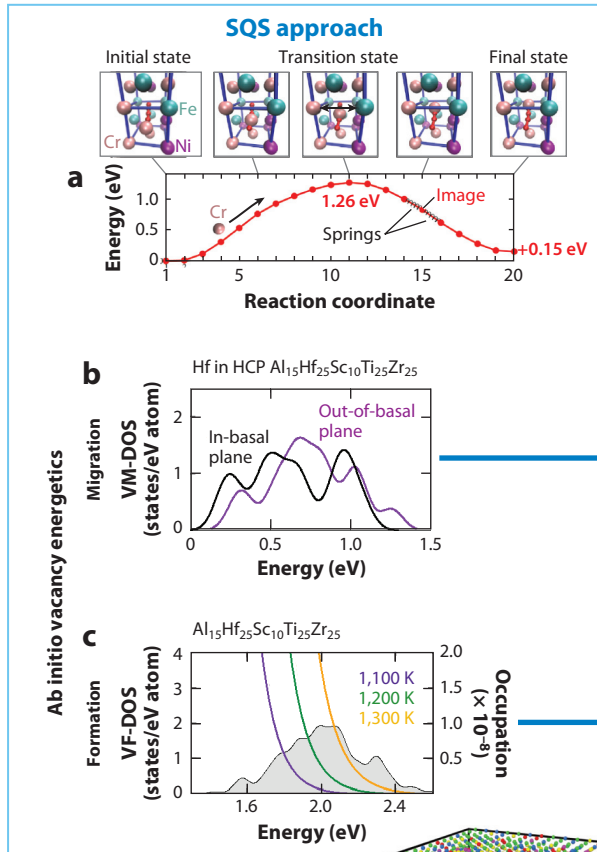
**6.1.1. Special quasirandom structures approach.** To fully retain the DFT accuracy, the most straightforward approach is, in principle, to perform explicit DFT calculations for structures or supercells containing defects for all different chemical arrangements. The immense number of configurations prohibits such a brute-force exploration; for example, in a five-component FCC HEA there are  $5^{12} \approx 2 \times 10^8$  configurations for the nearest-neighbor shell of a vacancy (taking symmetry into account may reduce this number slightly). As HEAs generally exhibit single-phase random solid solutions at compositions and temperatures where diffusion is experimentally measured, the widely used special quasirandom structure (SQS) approach (71) is ideal to mimic randomness and efficiently sample the configuration space. The benefit of the SQS approach is that, since the SQSs reproduce the most important correlations in a random mixture, the configuration space explored by SQSs represents the most probable chemical environments that defects may encounter in randomly disordered alloys. These states provide the dominant contributions to the thermal properties.

As the concentration of defects (especially vacancies) at thermal equilibrium is generally very low, it is reasonable to ignore interactions among defects. As a consequence, within the SQS approach, a single defect is generally introduced by removing (for vacancies) or adding (for impurities) an atom at one of the possible sites. The resulting defect supercell is subjected to self-consistent DFT relaxations to obtain the total energies, including local lattice distortions. To achieve statistical sampling, this procedure is repeated for other defect sites in the same SQS supercell. For the defect migration energies, the DFT-based nudged elastic band method (72, 73) is applied to two endpoints of the diffusion pathway that are connected by an elastic band including several artificially determined intermediate images in order to locate the saddle point, as illustrated in **Figure 5a** for ternary CrNiFe alloys.

By sufficiently sampling many defect energy states, the defect DOS corresponding to the energetic property of interest can be obtained, as exemplified in **Figure 5b,c**. With the knowledge of the defect DOS, effective properties at finite temperatures can be extracted accordingly. For defect formation energies, previous studies have shown that a statistical analysis is required as the sampled energy states are not activated equally at finite temperatures (22, 74). The temperature-dependent configurational excitations of defects result in negative excess formation entropies (74). The temperature-dependent defect concentrations exhibit a non-Arrhenius behavior (22, 74).

**6.1.2. Cluster expansion technique.** The *ab initio*-based cluster expansion (CE) technique has proven to be a very efficient and accurate tool for modeling alloy thermodynamics. It belongs to the category of lattice gas models with generalized mean-field approximations. Utilizing *ab initio* DFT energies as input, configuration-dependent energetic properties can be mapped onto

Configurational degrees of freedom



kMC

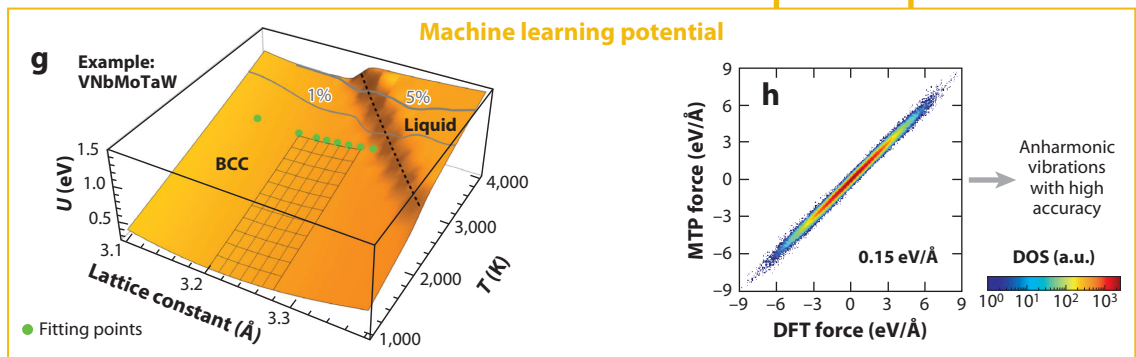
$$D^* = \frac{\langle R^2 \rangle}{6t}$$

$D^I = L \cdot \Phi$

Macro-diffusion coefficient

$$\tilde{D} = \sum_i D_i^I$$

Vibrational degrees of freedom



(Caption appears on following page)

**Figure 5** (Figure appears on preceding page)

Ab initio simulations of diffusion in HEAs. (a) Atomistic simulation of VM barriers in CrNiFe alloys using the nudged elastic band method. (b) VM-DOS of Hf and (c) VF-DOS in the HCP  $\text{Al}_{15}\text{Hf}_{25}\text{Sc}_{10}\text{Ti}_{25}\text{Zr}_{25}$  alloy. (d) CE for diffusion barriers. (e) Correlation of the DFT versus CE for KRA barriers and (f) for end-point energies. (g) Internal energy surfaces,  $U$ , as a function of lattice constant/volume and temperature,  $T$ , for MTP. (h) Correlation of the DFT forces versus MTP forces at 3000 K. (i) Vacancy PES and kMC simulations for various diffusivities. Abbreviations: BCC, body-centered cubic; CE, cluster expansion; DFT, density-functional theory; DOS, density of states; HCP, hexagonal close-packed; HEAs, high-entropy alloys; KRA, kinetically resolved activation; MTP, moment tensor potential; PES, potential energy surface; kMC, kinetic Monte Carlo; SQS, special quasirandom structure; VF, vacancy formation; VM, vacancy migration. Panels *b* and *c* adapted with permission from Reference 74. Panel *d* adapted with permission from Reference 80. Panels *g* and *h* adapted with permission from Reference 83.

Ising-like Hamiltonians with effective cluster interactions (ECIs). Several approaches are available to search for a good CE and to extract the corresponding ECIs, as summarized in Reference 75. Once a well-optimized CE is obtained, the associated ECIs can be used to predict the energies of arbitrary configurations at low computational cost.

The CE technique was mainly developed to address phase stabilities related to order-disorder transitions and phase diagrams in binary alloys. Later, with the development of the local CE approach as well as the concept of the kinetically resolved activation barriers, Van der Ven et al. investigated vacancies and interdiffusion in the  $\text{Li}_x\text{CoO}_2$  system (76) and binary Al-Li alloys (77, 78). By treating vacancies as an additional element, Zhang & Sluiter (79) derived a statistical model coupled with a full ternary CE to study vacancy properties in disordered concentrated Cu-Ni alloys. Although mainly applied to low-order systems, these successful extensions of the CE to diffusion energetics indicate the power of the CE to further model diffusion kinetics in multi-component and multiprincipal element systems. The applications of the CE to multicomponent diffusion, such as diffusion in HEAs, are limited due to the fact that the complexity of the CE parametrization significantly increases with an increasing number of components, and obtaining a good multicomponent CE becomes nontrivial. Instead of a direct brute-force search in a multicomponent clusters pool, Zhang & Sluiter (75) proposed a hierarchical approach to building up a multinary CE from ECIs of the subsystems using the inheritance of expansion coefficients concept. Such a promising feature may significantly reduce the difficulty of generating multicomponent CEs and provide a systematic way to establish the ab initio alloy database analogous to the well-known CALPHAD approach. For vacancy migration barriers, it has been shown that special treatment, namely the introduction of the pseudoatomic pair (as illustrated in **Figure 5d**), of the saddle-point configuration is necessary in order to retain the lattice gas assumption (75, 80).

## 6.2. Accurate Vibrational Free Energies from Machine Learning Potentials

The aforementioned defect configurational energetics does not include thermal vibration contributions. In reality, the diffusion processes (reorganizations of atoms) at elevated temperatures are coupled with thermal excitations (atomic vibrations, electronic excitations, etc.). Due to the time scales of thermal vibrations and diffusion being quite different, the vibrational contributions to the energetic properties can be evaluated for a fixed atomic configuration. Nevertheless, ab initio calculations of the full temperature-dependent vibrational free energy, including anharmonicity for a given atomic configuration, with defects are highly demanding (81). With the aid of the recently developed moment tensor potentials (MTPs), which are machine learning-based interatomic potentials, Grabowski et al. (82) have developed an efficient computational framework based on the two-stage upsampled thermodynamic integration using a Langevin dynamics approach (83) for an efficient and accurate calculation of the full vibrational free energy of disordered multicomponent alloys. The MTPs have proven to be robust for describing different phases for a wide temperature and volume range, as shown in **Figure 5g**. The strong correlation of the DFT forces with

**ECI:** effective cluster interaction

the molecular dynamics (MD) forces predicted by MTPs highlights the excellent performance of MTP (see **Figure 5b**).

### 6.3. Diffusion Coefficients from Kinetic Monte Carlo Simulations

Fundamentally, diffusion processes at the atomic scale can be described as a sequence of individual exchanges of vacancies with neighboring atoms or migrations of interstitial impurity atoms. With the knowledge of the potential energy associated with each local minimum as well as the defect migration barriers, that is, the potential energy surface on which the diffusing defects travel (illustrated in **Figure 5i**), diffusion coefficients can be calculated by monitoring the mean squared displacements of different diffusing elements as a function of time in, for example, kinetic Monte Carlo (kMC) or MD simulations. All energetics required for describing the potential energy surface of diffusion in kMC can be provided via the CE parameterizations described in Section 6.1.2. In general, according to the formulas derived by Allnatt (84), the phenomenological Onsager coefficients  $L_{ij}$  can be calculated from the ensemble average of the correlated fluctuations of species  $i$  and  $j$ , that is,

$$L_{ij} = \frac{\langle R_i R_j \rangle}{2dt}, \quad 9.$$

where  $d$  is the lattice dimension,  $t$  is the time,  $R_{i(j)} = \sum_{k=1}^N r_{i(j)}^k$  with  $r_{i(j)}^k$  the displacement of the  $k$ th atom of species  $i(j)$  and  $N$  the total number of species  $i(j)$ . By ignoring the cross correlations between different atoms, the Einstein formula for the tracer diffusion coefficient of species  $i$  is obtained,

$$D_i^* = \frac{\langle R_i^2 \rangle}{2dt}. \quad 10.$$

In order to compute the intrinsic diffusion coefficients and the interdiffusion coefficients, according to Equation 4, thermodynamic factors—the second derivative of the free energy with respect to the element concentrations—have to be evaluated first. In addition to the direct computation of the second derivatives, it has been shown that, for binaries, the grand canonical Monte Carlo simulation is an alternative approach for computing the thermodynamic factors (85).

The results of kMC simulations can be used to directly calculate the vacancy and atomic correlation factors (13, 15, 19). Using the random alloy model, these correlation factors have been determined for the equiatomic FCC CoCrFeMnNi alloy (13). The vacancy correlation factor was found to be less than unity, about 0.75 to 0.8 in the temperature interval of 1,000 K to 1,373 K (13). Such a value is consistent with some sluggishness of diffusion in FCC HEAs with respect to the pure elements, though the analysis is still absent for BCC and HCP multiprincipal element alloys.

## 7. CALPHAD MODELING OF MULTICOMPONENT DIFFUSION

Within the past 30 years, the CALPHAD method has extended to mobility databases and was successfully applied to assess diffusion data following the phenomenological methodology, similar to the thermodynamic description of Gibbs free energy for the calculation of phase diagrams. Most importantly, the CALPHAD approach allows the extrapolation of the multicomponent diffusion data to unknown composition regions. A detailed overview of CALPHAD-type modeling of kinetic databases was given by Zhang & Chen (86). In this section, we discuss recent advances in the modeling.

Before discussing the advances, however, several major limitations for the implementation of the CALPHAD method for diffusion processes have to be mentioned. First, the Darken

---

**MD:** molecular dynamics

**kMC:** kinetic Monte Carlo

---

approximation is followed for fluxes in a lattice-fixed reference frame. This approximation ignores all the jump correlation effects and can be applied only to the vacancy mechanism in the alloys with atomic mobilities that do not differ much from each other (moreover, the vacancy sources and sinks are not taken into account explicitly). This does not apply to intermetallic systems, where the diffusion rates of constituting elements can differ by orders of magnitude (37), and other (nonmonovacancy) diffusion mechanisms. The second severe limitation is the simplification of the kinetic part of the interdiffusion problem, despite taking into account the influence of the vacancy wind (87). Since the thermodynamic part strongly influences the results, it is always necessary to make some corrections to the thermodynamic parameters to ensure the correct effect of the thermodynamic data.

There have been three main directions of the development of the CALPHAD-type mobility databases in recent years. First is the thermodynamic assessment coupled with the interdiffusion coefficients extracted from diffusion couple and diffusion triple experiments (88). Second is a new high-throughput technique of diffusion multiples coupled with the inverse numerical method (89). Third is the direct extraction of the mobility parameters from the tracer diffusion experiments (90).

In References 91–93, calorimetric experiments and ab initio calculations of end-member Gibbs energies were used to assess the thermodynamic properties of ternary Ni and binary and ternary Ti alloys. Then, diffusion couples in conjunction with a new thermodynamic database assessment were used to assess the atomic mobilities and CALPHAD-type mobility parameters. Diffusion couples of Ti triple systems were utilized to develop a self-consistent atomic mobility database in the works of Bai et al. (94, 95), Wei et al. (96), and Dong et al. (97). Interdiffusion coefficients were extracted by the Whittle–Green method (98) and tracer diffusion coefficients by the Hall method (40). Diffusion couple experiments in the Fe–Al–(Si, Mn) BCC systems were used to optimize the mobilities of the impurities in Al, Si, and Mn (99). Similar experiments were carried out to extract the interdiffusion coefficients and impurity diffusion coefficients for the Mg–Li–Al system (100). The assessment of the thermodynamic parameters and mobility parameters was performed using the diffusion couple and diffusion triple experiments in the recent work of Xia et al. (88) in the Co–Fe–Ni system. The interdiffusion coefficients were extracted by the Sauer–Freise method (40). In all present works the diffusion-controlled transformations (DICTRA) software within ThermoCalc (<https://thermocalc.com>) was used to assess the mobility parameters from the chemical diffusion coefficients.

The concept of a diffusion multiple was recently developed by Zhao et al. (101) and has an order-of-magnitude-higher efficiency in comparison with diffusion couples. More details of this can be seen in the review paper by Zhong et al. (102). Recently, the diffusion multiple method was used by Chen & Zhang (103) to assess the atomic mobilities in Fe–Mn–Si systems (89) and five-component HEAs. The interdiffusivity matrices, depending on the composition, were prepared using the pragmatic inverse numerical method. The vacancy-wind effect was also taken into account. The authors used the end-member atomic mobility parameters known from the literature in order to assess the binary and ternary interaction parameters. In addition, the transformation relations between diffusivities with different reference elements were developed, which are helpful for multiprincipal element alloys. With respect to the application to HEAs, a mobility database was also developed using data from the literature and validated by diffusion experiments in the work of Zhang et al. (104).

Despite the high efficiency of the diffusion multiple method, the definition of the atomic mobility parameters from interdiffusion coefficients is not very accurate, as discussed before, because the results depend on the thermodynamic description of the system (88). In contrast, tracer diffusion experiments allow for defining the mobility directly from the intrinsic diffusion coefficients

## ASSESSMENT OF MOBILITY PARAMETERS

For automated assessment of the mobility parameters, see open-access software **PyMob**: <http://www.icams.de/content/software-development>.

using the Einstein relation and do not depend on the choice of thermodynamic database. Moreover, tracer diffusion coefficients can give important information about physical effects of the diffusion, such as the effect of impurities or vacancies on the mobility of matrix components. For example, tracer diffusion experiments were recently carried out by Gheno et al. (105) for Cr and Ni in a Ni–Cr alloy, and the corresponding mobility parameters for the Ni–Cr system were reassessed. Furthermore, a physical effect of the vacancy–solute exchange mechanism was found and studied.

A new method yet to be reported is the automated assessment of the mobility parameters from tracer diffusion experiments using the software **PyMob** (<http://www.icams.de/content/software-development>), developed by Abrahams et al. (90). A raw database of tracer diffusion coefficients is adopted to extract a database of mobility parameters (see the sidebar titled Assessment of Mobility Parameters). The parameters are assessed step by step from the end-members to the ternary interactions. The software allows for quickly updating the database when new raw data become available. To choose the model variant with the corresponding mobility parameters, the **PyMob** software uses statistical criteria, namely the Bayesian information criterion and Akaike information criterion, to choose the model with or without ternary interactions. Note that **DICTRA** software also allows for assessing the mobility parameters from different diffusion experiments, but one should learn how to implement the software for a specific case. For unknown end-member parameters, for example, for self-diffusion of Cr in a (metastable) FCC lattice, one can use the values calculated ab initio or by MD simulations.

As a last comment, we would like to highlight the revision of the pair-exchange concept (106), which was applied together with the experimental tracer diffusion coefficients (see Section 5) to validate the thermodynamic database for HEAs applied to diffusion couple experiments (62). The pair-exchange formulation allows, in the framework of **CALPHAD**, a unique definition of the diffusion coefficients of multicomponent systems without specifying a reference chemical potential. Therefore, the formal challenges to describing the multiprincipal element systems seem to be resolved.

## 8. SUMMARY AND CONCLUDING REMARKS

Tracer and intrinsic diffusion coefficients are the basic quantities required for a quantitative understanding of the mass transport phenomena and diffusional interactions between components in complex multicomponent material systems including multiprincipal element and compositionally complex alloys. In this review, the latest developments related to the determination of these diffusion parameters from experimental, numerical-inverse, and ab initio-informed methods have been discussed comprehensively.

The radiotracer method is a traditional and, in principle, straightforward technique for measuring the tracer diffusion coefficients of components in (typically homogeneous) alloys with fixed composition. The recently developed radiotracer-interdiffusion couple technique presents an advanced and unique approach to measure the concentration-dependent tracer diffusion coefficients in multicomponent alloys, paving the way for a high-throughput determination of atomic mobilities. However, the tracer method faces serious problems with its application to several important

constituting elements such as Al, Ga, and Si because of the unavailability, short lifetimes, and high costs of the corresponding radioisotopes. Further, the usage of the radiotracer technique is nowadays limited due to stringent safety regulations.

The diffusion couple method is, therefore, a widely practiced alternative. It used to be common textbook knowledge that, with the diffusion couple method, tracer and intrinsic diffusion coefficients could be estimated only for binary systems. For ternary systems, only the interdiffusion coefficients were accessible and no analytic expressions existed for the determination of the basic diffusion coefficients in systems with more than three components,  $n > 3$ . Nowadays, the recently proposed PB method can be used to experimentally determine the tracer and main intrinsic diffusion coefficients of the components at the Kirkendall marker plane in an arbitrary multicomponent system. Tracer, main, and cross intrinsic diffusion coefficients can be estimated by extending the Kirkaldy–Lane method proposed for ternary systems to PT and BD diffusion couples in multicomponent systems utilizing the thermodynamic details at the cross of the diffusion paths. Only two diffusion profiles are required irrespective of the number of components in an  $n > 2$  component system.

The combined radiotracer-interdiffusion couple method can be extended to PB, PT, or BD diffusion couple methods for estimating the composition-dependent tracer and intrinsic diffusion coefficients for the whole composition interval of the diffusion path that develops during the measurement. Knowing the thermodynamic details, the tracer and intrinsic diffusion coefficients of the components for which suitable radioisotopes are not available can be further determined. The experimental methods, being most suitable for homogeneous single-phase alloys, have their limitations and encounter obvious difficulties when applied to phase mixtures. Moreover, the generation of composition-dependent diffusion parameters for all constituent components over a wide homogeneity range is not an easy task. As described, the PB, PT, and BD methods work only when the diffusion profiles can be generated and may be restricted to a particular (rather than the entire) composition range of a system.

In the absence of available data or suitable experimental methods in a multicomponent system, the solution to determining the interdiffusion matrix in the numerical inverse method was previously established by using just the measured concentration profiles. This was a serious drawback in the absence of the uniqueness of the solution. Today, these methods can be combined with experimental methods to develop a reliable mobility database in complex material systems by comparing the measured profiles with the experimentally estimated tracer and intrinsic diffusion coefficients (66). Following this route, one can extract the data in a composition range in which the data cannot be estimated experimentally. In its current formulation, the ThermoCalc-DICTRA method does not consider the contributions of the vacancy-wind effect, which may play a crucial role, and an alternate method is desirable. Recent advances in CALPHAD modeling of mobility databases for multicomponent alloys, including HEAs, and the new experimental methods and numerical techniques, which in principle can also consider the vacancy-wind effect, were briefly described.

Ab initio DFT-based simulations have recently advanced to guide the design of novel multi-principal element alloys, such as by predicting phase transitions and simulating diffusion properties. The main challenge lies in the fact that both highly complex chemical and vibrational degrees of freedom need to be properly taken into account, requiring new methodological developments. We have shown in this review that the chemical degrees of freedom can be well tackled by highly optimized multicomponent cluster expansions. Critical experimentally measurable diffusion coefficients, such as tracer and intrinsic diffusivities, can be extracted from direct kMC simulations or from the concentration profile analysis obtained from kMC. For the vibrational degrees of freedom, thermodynamic properties up to the melting point of HEAs can be efficiently calculated by the recently developed machine learning potentials with DFT accuracy. Most importantly,

ab initio simulations at the atomic scale provide physical insight into the interplay between phase stabilities and diffusion kinetics. On the one hand, the change of the chemical order may have significant impact on the diffusion kinetics, such as ultrafast diffusion. On the other hand, interestingly, the specific diffusion kinetics may also result in different chemical short-range or long-range ordering.

To summarize, no method on its own is enough to establish a reliable mobility database in a multicomponent alloy system of practical importance. A combination of experimental, numerical-inverse, and DFT methods, as described in this review article, should be utilized to establish a reliable mobility database and understanding of the complex diffusional interactions between components in order to simulate the microstructural evolution or to understand various physical and mechanical properties of materials.

## DISCLOSURE STATEMENT

The authors are not aware of any affiliations, memberships, funding, or financial holdings that might be perceived as affecting the objectivity of this review.

## ACKNOWLEDGMENTS

A.P. acknowledges financial support from the Aeronautics Research and Development Board, India, grant number ARDB/GTMAP/01/2031786/M. Financial support from the Deutsche Forschungsgemeinschaft via the research projects DI 1419/13-2, DI 1419/17-1, GR 3716/5-1, and STE 116/30-1/2 is gratefully acknowledged. B.G. acknowledges funding from the European Research Council under the EU's Horizon 2020 Research and Innovation Programme (grant 865855) and support by the Stuttgart Center for Simulation Science (SimTech).

## LITERATURE CITED

1. Miracle D, Senkov O. 2017. A critical review of high entropy alloys and related concepts. *Acta Mater.* 122:448–511
2. Cantor B, Chang ITH, Knight P, Vincent AJB. 2004. Microstructural development in equiatomic multicomponent alloys. *Mater. Sci. Eng. A* 375–377:213–18
3. Senkov O, Scott J, Senkova S, Miracle D, Woodward C. 2011. Microstructure and room temperature properties of a high-entropy TaNbHfZrTi alloy. *J. Alloys Compd.* 509:6043–48
4. Feuerbacher M, Lienig T, Thomas C. 2018. A single-phase bcc high-entropy alloy in the refractory Zr–Nb–Ti–V–Hf system. *Scr. Mater.* 152:40–43
5. Feuerbacher M, Heidelmann M, Thomas C. 2016. Hexagonal high-entropy alloys. *Mater. Res. Lett.* 3:1–6
6. Rogal L, Bobrowski P, Körmann F, Divinski S, Stein F, Grabowski B. 2017. Computationally-driven engineering of sublattice ordering in a hexagonal AlHfScTiZr high entropy alloy. *Sci. Rep.* 7:2209
7. Yeh J, Chen S, Lin S, Gan J, Chin T, et al. 2004. Nanostructured high-entropy alloys with multiple principal elements: novel alloy design concepts and outcomes. *Adv. Eng. Mater.* 6:299–303
8. Divinski SV, Lukianova OA, Wilde G, Dash A, Esakiraja N, Paul A. 2022. High-entropy alloys: diffusion. In *Encyclopedia of Materials*, Vol. 2, ed. G Miyamoto, MC Gao, pp. 402–16. Amsterdam: Elsevier
9. Dabrowa J, Zajusz M, Kucza W, Cieslak G, Berent K, et al. 2019. Demystifying the sluggish diffusion effect in high entropy alloys. *J. Alloys Compd.* 783:193–207
10. Mehta A, Sohn Y. 2021. Investigation of sluggish diffusion in FCC Al<sub>0.25</sub>CoCrFeNi high-entropy alloy. *Mater. Res. Lett.* 9(5):239–46
11. Mehrer H. 1990. *Diffusion in Solids: Fundamentals, Methods, Materials, Diffusion-Controlled Processes*. Berlin: Springer
12. Vaidya M, Pradeep K, Murty B, Wilde G, Divinski S. 2018. Bulk tracer diffusion in CoCrFeNi and CoCrFeMnNi high entropy alloys. *Acta Mater.* 146:211–24

13. Gaertner D, Kottke J, Chumlyakov Y, Hergemöller F, Wilde G, Divinski SV. 2020. Tracer diffusion in single crystalline CoCrFeNi and CoCrFeMnNi high-entropy alloys: kinetic hints towards a low-temperature phase instability of the solid-solution? *Scr. Mater.* 187:57–62
14. Paul A, Laurila T, Vuorinen V, Divinski SV. 2014. *Thermodynamics, Diffusion and the Kirkendall Effect in Solids*. Cham, Switz.: Springer
15. Murch GE, Thorn RJ. 1979. Calculation of the diffusion correlation factor by Monte Carlo methods. *Philos. Mag. A* 39:673–77
16. Mizuno M, Sugita K, Araki H. 2019. Defect energetics for diffusion in CrMnFeCoNi high-entropy alloy from first-principles calculations. *Comput. Mater. Sci.* 170:109163
17. Quyang H, Fultz B. 1989. Percolation in alloys with thermally activated diffusion. *J. Appl. Phys.* 66:4752–55
18. Mehrer H, ed. 1990. *Diffusion in Metals and Alloys*. Berlin: Springer
19. Kottke J, Utt D, Laurent-Brocq M, Fareed A, Gaertner D, et al. 2020. Experimental and theoretical study of tracer diffusion in a series of (CoCrFeMn)<sub>100-x</sub>Ni<sub>x</sub> alloys. *Acta Mater.* 194:236–48
20. Vaidya M, Trubel S, Murty B, Wilde G, Divinski S. 2016. Ni tracer diffusion in CoCrFeNi and CoCrFeMnNi high entropy alloys. *J. Alloys Compd.* 688:994–1001
21. Nadutov V, Mazanko V, Makarenko S. 2017. Tracer diffusion of cobalt in high-entropy alloys Al<sub>x</sub>FeNiCoCuCr. *Metallofiz. Noveishie Tekhnologii* 39:337–48
22. Vaidya M, Sen S, Zhang X, Frommeyer L, Rogal L, et al. 2020. Phenomenon of ultra-fast tracer diffusion of Co in HCP high entropy alloys. *Acta Mater.* 196:220–30
23. Maier K, Mehrer H, Lessmann E, Schuele W. 1976. Self-diffusion in nickel at low temperatures. *Phys. Status Solidi B* 78:689–98
24. James D, Leak G. 1966. Self-diffusion and diffusion of cobalt in alpha and delta-iron. *Philos. Mag.* 14:701–13
25. Hood G, Zou H, Schultz R, Matsuura N, Roy J, Jackman J. 1997. Self- and Hf diffusion in  $\alpha$ -Zr and in dilute, Fe-free, Zr(Ti) and Zr(Nb) alloys. *Defect Diffus. Forum* 143:49–54
26. Million B, Růžičková J, Velíšek J, Vřešťál J. 1981. Diffusion processes in the Fe–Ni system. *Mater. Sci. Eng.* 50(1):43–52
27. Iijima Y, Kimura K, Lee CG. 1995. Self-diffusion in B.C.C. and ordered phases of an equiatomic iron–cobalt alloy. *Acta Metal. Mater.* 43:1183–88
28. Zhang J, Muralikrishna GM, Asabre A, Kalchev Y, Müller J, et al. 2021. Tracer diffusion in the  $\sigma$  phase of the CoCrFeMnNi system. *Acta Metall.* 203:116498
29. Frank S, Södervall U, Herzig C. 1995. Self-diffusion of Ni in single and polycrystals of Ni<sub>3</sub>Al. A study of SIMS and radiotracer analysis. *Phys. Status Solidi B* 191:45–55
30. Knorr K, Macht M, Freitag K, Mehrer H. 1999. Self-diffusion in the amorphous and supercooled liquid state of the bulk metallic glass Zr<sub>46.75</sub>Ti<sub>8.25</sub>Cu<sub>7.5</sub>Ni<sub>10</sub>Be<sub>27.5</sub>. *J. Non-Cryst. Solids* 250–252(2):669–73
31. Kötstler C, Faupel F, Hehenkamp T. 1986. Carbon-vacancy binding in Ni–C alloys. *Scr. Metall.* 20:1755–59
32. Chen T, Tiwari GP, Iijima Y, Yamauchi K. 2003. Volume and grain boundary diffusion of chromium in Ni-base Ni–Cr–Fe alloys. *Mater. Trans.* 44(1):40–46
33. Lukianova O, Rao Z, Kulitckii V, Li Z, Wilde G, Divinski S. 2020. Impact of interstitial carbon on self-diffusion in CoCrFeMnNi high entropy alloys. *Scr. Mater.* 188:264–68
34. Herzig C, Willecke R, Viergege K. 1991. Self-diffusion and fast cobalt impurity diffusion in the bulk and in grain boundaries of hexagonal titanium. *Philos. Mag. A* 63:949–58
35. Wang Q, Lu Y, Yu Q, Zhang Z. 2018. The exceptional strong face-centered cubic phase and semi-coherent phase boundary in a eutectic dual-phase high entropy alloy AlCoCrFeNi. *Sci. Rep.* 8:14910
36. Tsai K, Tsai M, Yeh J. 2013. Sluggish diffusion in Co–Cr–Fe–Mn–Ni high-entropy alloys. *Acta Mater.* 61:4887–97
37. Divinski S. 2017. Defects and diffusion in ordered compounds. In *Handbook of Solid State Diffusion*, Vol. 1: *Diffusion Fundamentals and Techniques*, ed. A Paul, SV Divinski, pp. 449–518. Amsterdam: Elsevier
38. He QF, Ye YF, Yang Y. 2017. Formation of random solid solution in multicomponent alloys: from Hume-Rothery rules to entropic stabilization. *J. Phase Equilib. Diffus.* 38:416–25

39. Faupel F, Frank W, Macht MP, Mehrer H, Naundorf V, et al. 2003. Diffusion in metallic glasses and supercooled melts. *Rev. Modern Phys.* 75:237–80
40. Paul A, Divinski S, eds. 2017. *Handbook of Solid State Diffusion*, Vol. 1: *Diffusion Fundamentals and Techniques*. Amsterdam: Elsevier
41. Manning JR. 1970. Cross terms in the thermodynamic diffusion equations for multicomponent alloys. *Metall. Mater. Trans. B* 1(2):499–505
42. Manning J. 1967. Diffusion and the Kirkendall shift in binary alloys. *Acta Metall.* 15(5):817–26
43. Darken LS. 1948. Diffusion, mobility and their interrelation through free energy in binary metallic systems. *Trans. AIME* 175:184–201
44. Le Claire AD. 1958. Random walks and drift in chemical diffusion. *Philos. Mag.* 3(33):921–39
45. Onsager L. 1931. Reciprocal relations in irreversible processes. II. *Phys. Rev.* 38(12):2265–79
46. Onsager L. 1945. Theories and problems of liquid diffusion. *Ann. N. Y. Acad. Sci.* 46(5):241–65
47. Esakkiraja N, Dash A, Mondal A, Hary Kumar K, Paul A. 2021. Correlation between estimated diffusion coefficients from different types of diffusion couples in multicomponent system. *Materialia* 16:101046
48. Kirkaldy JS, Young DJ. 1987. *Diffusion in the Condensed State*. London: Inst. Met.
49. Kirkaldy J, Lane J. 1966. Diffusion in multicomponent metallic systems: IX. Intrinsic diffusion behavior and the Kirkendall effect in ternary substitutional solutions. *Can. J. Phys.* 44(9):2059–72
50. Cserháti C, Ugaste Ü, van Dal MJH, Lousberg NJHGM, Kodentsov AA, van Loo FJJ. 2001. On the relation between interdiffusion and tracer diffusion coefficients in ternary solid solutions. *Defect Diffus. Forum* 194:189–94
51. Paul A. 2013. A pseudobinary approach to study interdiffusion and the Kirkendall effect in multicomponent systems. *Philos. Mag.* 93(18):2297–315
52. Esakkiraja N, Pandey K, Dash A, Paul A. 2019. Pseudo-binary and pseudo-ternary diffusion couple methods for estimation of the diffusion coefficients in multicomponent systems and high entropy alloys. *Philos. Mag.* 99:2236–64
53. Dash A, Esakkiraja N, Paul A. 2020. Solving the issues of multicomponent diffusion in an equiatomic NiCoFeCr medium entropy alloy. *Acta Mater.* 193:163–71
54. Paul A. 2017. Comments on “Sluggish diffusion in Co–Cr–Fe–Mn–Ni high-entropy alloys” by K.Y. Tsai, M.H. Tsai and J.W. Yeh, *Acta Materialia* 61 (2013) 4887–4897. *Scr. Mater.* 135:153–57
55. Esakkiraja N, Gupta A, Jayaram V, Hickel T, Divinski SV, Paul A. 2020. Diffusion, defects and understanding the growth of a multicomponent interdiffusion zone between Pt-modified B2 NiAl bond coat and single crystal superalloy. *Acta Mater.* 195:35–49
56. Kiruthika P, Paul A. 2015. A pseudo-binary interdiffusion study in the  $\beta$ -Ni (Pt) Al phase. *Philos. Mag. Lett.* 95(3):138–44
57. Kiruthika P, Makineni S, Srivastava C, Chattopadhyay K, Paul A. 2016. Growth mechanism of the interdiffusion zone between platinum modified bond coats and single crystal superalloys. *Acta Mater.* 105:438–48
58. DeHoff R, Kulkarni N. 2002. The trouble with diffusion. *Mater. Res.* 5(3):209–29
59. Morral JE. 2018. Body-diagonal diffusion couples for high entropy alloys. *J. Phase Equilib. Diffus.* 39(1):51–56
60. Verma V, Tripathi A, Venkateswaran T, Kulkarni KN. 2020. First report on entire sets of experimentally determined interdiffusion coefficients in quaternary and quinary high-entropy alloys. *J. Mater. Res.* 35(2):162–71
61. Esakkiraja N, Paul A. 2018. A novel concept of pseudo ternary diffusion couple for the estimation of diffusion coefficients in multicomponent systems. *Scr. Mater.* 147:79–82
62. Gaertner D, Abrahams K, Kottke J, Esin VA, Steinbach I, et al. 2019. Concentration-dependent atomic mobilities in FCC CoCrFeMnNi high-entropy alloys. *Acta Mater.* 166:357–70
63. Zhong J, Chen L, Zhang L. 2021. Automation of diffusion database development in multicomponent alloys from large number of experimental composition profiles. *NPJ Comput. Mater.* 7:35
64. Mehta A, Belova I, Murch G, Sohn Y. 2021. Measurement of interdiffusion and tracer diffusion coefficients in FCC Co-Cr-Fe-Ni multi-principal element alloy. *J. Phase Equilib. Diffus.* 42:696–707
65. Belova I, Sohn Y, Murch G. 2015. Measurement of tracer diffusion coefficients in an interdiffusion context for multicomponent alloys. *Philos. Mag. Lett.* 95:416–24

66. Kumar H, Dash A, Paul A, Bhattacharyya S. 2022. A physics-informed neural network-based numerical inverse method for optimization of diffusion coefficients in NiCoFeCr multi principal element alloy. *Scr. Mater.* 214:114639
67. Manning JR. 1959. Tracer diffusion in a chemical concentration gradient in silver-cadmium. *Phys. Rev.* 116:69–80
68. Meyer R, Sliifkin L. 1966. Activity coefficient and vacancy-flow effects on diffusion in silver-gold alloys. *Phys. Rev.* 149:556–63
69. Belova I, Kulkarni N, Sohn Y, Murch G. 2014. Simultaneous tracer diffusion and interdiffusion in a sandwich-type configuration to provide the composition dependence of the tracer diffusion coefficients. *Philos. Mag.* 94:3560–73
70. Muralikrishna G, Tas B, Esakiraja N, Esin V, Hari Kumar K, et al. 2021. Composition dependence of Fe tracer diffusion coefficients in Fe–Ga alloys: a case study by a tracer-interdiffusion couple method. *Acta Mater.* 203:116446
71. Zunger A, Wei SH, Ferreira LG, Bernard JE. 1990. Special quasirandom structures. *Phys. Rev. Lett.* 65(3):353–56
72. Henkelman G, Uberuaga BP, Jónsson H. 2000. A climbing image nudged elastic band method for finding saddle points and minimum energy paths. *J. Chem. Phys.* 113(22):9901–4
73. Henkelman G, Jónsson H. 2000. Improved tangent estimate in the nudged elastic band method for finding minimum energy paths and saddle points. *J. Chem. Phys.* 113(22):9978–85
74. Zhang X, Divinski SV, Grabowski B. 2022. *Ab initio* prediction of vacancy energetics in HCP Al–Hf–Sc–Ti–Zr high entropy alloys and the subsystems. *Acta Mater.* 227:117677
75. Zhang X, Sluiter MHF. 2016. Cluster expansions for thermodynamics and kinetics of multicomponent alloys. *J. Phase Equilib. Diffus.* 37(1):44–52
76. Van der Ven A, Ceder G, Asta M, Tepesch PD. 2001. First-principles theory of ionic diffusion with nondilute carriers. *Phys. Rev. B* 64(18):184307
77. Van der Ven A, Ceder G. 2005. Vacancies in ordered and disordered binary alloys treated with the cluster expansion. *Phys. Rev. B* 71(5):054102
78. Van der Ven A, Ceder G. 2005. First principles calculation of the interdiffusion coefficient in binary alloys. *Phys. Rev. Lett.* 94(4):045901
79. Zhang X, Sluiter MHF. 2015. *Ab initio* prediction of vacancy properties in concentrated alloys: the case of fcc Cu–Ni. *Phys. Rev. B* 91(17):174107
80. Zhang X, Sluiter MHF. 2019. Kinetically driven ordering in phase separating alloys. *Phys. Rev. Mater.* 3(9):095601
81. Zhang X, Grabowski B, Hickel T, Neugebauer J. 2018. Calculating free energies of point defects from *ab initio*. *Comput. Mater. Sci.* 148:249–59
82. Grabowski B, Ikeda Y, Srinivasan P, Körmann F, Freysoldt C, et al. 2019. *Ab initio* vibrational free energies including anharmonicity for multicomponent alloys. *NPJ Comput. Mater.* 5(1):80
83. Duff AI, Davey T, Korbmacher D, Glensk A, Grabowski B, et al. 2015. Improved method of calculating *ab initio* high-temperature thermodynamic properties with application to ZrC. *Phys. Rev. B* 91(21):214311
84. Allnatt AR. 1965. Theory of phenomenological coefficients in solid-state diffusion. I. General expressions. *J. Chem. Phys.* 43(6):1855–63
85. Van der Ven A, Yu HC, Ceder G, Thornton K. 2010. Vacancy mediated substitutional diffusion in binary crystalline solids. *Prog. Mater. Sci.* 55(2):61–105
86. Zhang L, Chen Q. 2017. CALPHAD-type modeling of diffusion kinetics in multicomponent alloys. In *Handbook of Solid State Diffusion*, Vol. 1, ed. A Paul, S Divinski, pp. 321–62. Amsterdam: Elsevier
87. Manning J. 1968. *Diffusion Kinetics for Atoms in Crystals*. Princeton, NJ: Van Nostrand
88. Xia CH, Wang Y, Wang JJ, Lu XG, Zhang L. 2021. Thermodynamic assessment of the Co–Fe–Ni system and diffusion study of its fcc phase. *J. Alloys Compd.* 853:157165
89. Deng S, Chen W, Zhong J, Zhang L, Du Y, Chen L. 2017. Diffusion study in bcc\_A2 Fe–Mn–Si system: experimental measurement and CALPHAD assessment. *Calphad* 56:230–40

90. Abrahams K, Zomorodpoosh S, Khorasgani AR, Roslyakova I, Steinbach I, Kundin J. 2021. Automated assessment of a kinetic database for fcc Co–Cr–Fe–Mn–Ni high entropy alloys. *Model. Simul. Mater. Sci. Eng.* 29:0550072
91. Zhao N, Liu W, Wang JJ, Lu XG, Zhang L. 2020. Thermodynamic assessment of the Ni–Co–Cr system and diffusion study of its fcc phase. *Calphad* 71:101996
92. Wang J, Zheng W, Xu G, Zeng X, Cui Y. 2020. Thermodynamic assessment of the Ti–Al–Zr system and atomic mobility of its bcc phase. *Calphad* 70:101801
93. Jinwan H, Yang W, Jingjing W, Xiao-Gang L, Lijun Z. 2018. Thermodynamic assessments of the Ni–Cr–Ti system and atomic mobility of its fcc phase. *J. Phase Equilib. Diffus.* 39:597–609
94. Bai W, Tian Y, Xu G, Yang Z, Liu L, et al. 2019. Diffusivities and atomic mobilities in bcc Ti–Zr–Nb alloys. *Calphad* 64:160–74
95. Bai W, Xu G, Tan M, Yang Z, Zeng L, et al. 2018. Diffusivities and atomic mobilities in bcc Ti–Mo–Zr alloys. *Materials* 11(10)
96. Wei Z, Wang C, Qin S, Lu Y, Yu X, Liu X. 2020. Assessment of atomic mobilities for bcc phase in the Ti–Nb–V system. *J. Phase Equilib. Diffus.* 41:191–206
97. Dong H, Wang J, Xu G, Zhou L, Cui Y. 2018. Assessment of atomic mobility for BCC Ti–Mn and Ti–Al–Mn alloys. *Calphad* 62:141–47
98. Whittle D, Green A. 1974. The measurement of diffusion coefficients in ternary system. *Scr. Metall.* 8:883–84
99. Zheng W, Wang J, He Y, Lu XG, Li L. 2018. Experimental and computational study of diffusion mobilities for the bcc phase in the Fe–Al–(Si, Mn) systems. *Calphad* 61:189–97
100. Christianson DW, Zhu L, Manuel MV. 2020. Experimental measurement of diffusion coefficients and assessment of diffusion mobilities in HCP Mg–Li–Al alloys. *Calphad* 71:101999
101. Zhao JC, Zheng X, Cahill DG. 2005. High-throughput diffusion multiples. *Mater. Today* 8(10):28–37
102. Zhong J, Chen L, Zhang L. 2020. High-throughput determination of high-quality interdiffusion coefficients in metallic solids: a review. *J. Mater. Sci.* 55:10303–38
103. Chen W, Zhang L. 2017. High-throughput determination of interdiffusion coefficients for Co–Cr–Fe–Mn–Ni high-entropy alloys. *J. Phase Equilib. Diffus.* 38:457–65
104. Zhang C, Zhang F, Jin K, Bei H, Chen S, et al. 2017. Understanding of the elemental diffusion behavior in concentrated solid solution alloys. *J. Phase Equilib. Diffus.* 38:434–44
105. Gheno T, Jomard F, Desgranges C, Martinelli L. 2018. Tracer diffusion of Cr in Ni and Ni–22Cr studied by SIMS. *Materialia* 3:145–52
106. Kundin J, Steinbach I, Abrahams K, Divinski SV. 2021. Pair-exchange diffusion model for multicomponent alloys revisited. *Materialia* 16:101047